National Library of Canada
Bibliothèque nationale du Canada

Canadian Theses Service
Service des thèses canadiennes

Ottawa, Canada
K1A 0N4

NOTICE

The quality of this microform is heavily dependent upon the quality of the original thesis submitted for microfilming. Every effort has been made to ensure the highest quality of reproduction possible.

If pages are missing, contact the university which granted the degree.

Some pages may have indistinct print especially if the original pages were typed with a poor typewriter ribbon or if the university sent us an inferior photocopy.

Reproduction in full or in part of this microform is governed by the Canadian Copyright Act, R.S.C. 1970, c. C-30, and subsequent amendments.

AVIS

La qualité de cette microforme dépend grandement de la qualité de la thèse soumise au microfilmage. Nous avons tout fait pour assurer une qualité supérieure de reproduction.

S'il manque des pages, veuillez communiquer avec l'université qui a conféré le grade.

La qualité d'impression de certaines pages peut laisser à désirer, surtout si les pages originales ont été dactylographiées à l'aide d'un ruban usé ou si l'université nous a fait parvenir une photocopie de qualité inférieure.

La reproduction, même partielle, de cette microforme est soumise à la Loi canadienne sur le droit d'auteur, SRC 1970, c. C-30, et ses amendements subséquents.

NL-339 (r. 88/04) c

Canada

UNIVERSITY OF ALBERTA

OPTOELECTRONIC MULTIPLEXING AND DEMULTIPLEXING

by

PIERRE F. TREMBLAY

A THESIS

SUBMITTED TO THE FACULTY OF GRADUATE STUDIES AND RESEARCH

IN PARTIAL FULFILLMENT OF THE REQUIREMENTS FOR THE DEGREE OF

MASTER OF SCIENCE

DEPARTMENT OF ELECTRICAL ENGINEERING

EDMONTON, ALBERTA

SPRING 1991

National Library of Canada
Bibliothèque nationale du Canada

Canadian Theses Service
Service des thèses canadiennes

Ottawa, Canada
K1A 0N4

The author has granted an irrevocable non-exclusive licence allowing the National Library of Canada to reproduce, loan, distribute or sell copies of his/her thesis by any means and in any form or format, making this thesis available to interested persons.

L'auteur a accordé une licence irrévocable et non exclusive permettant à la Bibliothèque nationale du Canada de reproduire, prêter, distribuer ou vendre des copies de sa thèse de quelque manière et sous quelque forme que ce soit pour mettre des exemplaires de cette thèse à la disposition des personnes intéressées.

The author retains ownership of the copyright in his/her thesis. Neither the thesis nor substantial extracts from it may be printed or otherwise reproduced without his/her permission.

L'auteur conserve la propriété du droit d'auteur qui protège sa thèse. Ni la thèse ni des extraits substantiels de celle-ci ne doivent être imprimés ou autrement reproduits sans son autorisation.

ISBN 0-315-66577-7

Canada

UNIVERSITY OF ALBERTA

RELEASE FORM

NAME OF AUTHOR: PIERRE F. TREMBLAY

TITLE OF THESIS: OPTOELECTRONIC MULTIPLEXING AND DEMULTIPLEXING

DEGREE: MASTER OF SCIENCE

YEAR THIS DEGREE GRANTED: 1991

Permission is hereby granted to THE UNIVERSITY OF ALBERTA LIBRARY to reproduce single copies of this thesis and to lend or sell such copies for private, scholarly, or scientific purposes only.

The author reserves other publication rights, and neither the thesis nor extensive extracts from it may be printed or otherwise reproduced without the author's written permission.

PERMANENT ADDRESS:
3873 MGR BÉGIN
JONQUIÈRE, QUÉBEC
CANADA, G7X 3T5

Date: December 7, 1990

UNIVERSITY OF ALBERTA

FACULTY OF GRADUATE STUDIES AND RESEARCH

The undersigned certify that they have read, and recommend to the Faculty of Graduate Studies and Research for acceptance, a thesis entitled OPTOELECTRONIC MULTIPLEXING AND DEMULTIPLEXING submitted by PIERRE F. TREMBLAY in partial fulfillment of the requirements for the degree of MASTER OF SCIENCE.

R.I. MacDonald

G.D. Cormack

C.G. Englefield

A.E. Kamal

Date: December 7, 1990

A Léandre, Maude, et Hélène.

ABSTRACT

The use of optoelectronic gates, passive optical delay lines, and switched photodetectors to perform optoelectronic time-division multiplexing and demultiplexing is examined.

An optoelectronic multiplexer was built that provided a multiplexed signal at a line rate of 560 Mb/s. Inexpensive CD type lasers were modulated to generate eight RZ optical data streams at a rate of 70 Mb/s and one stream of synchronization pulses with a repetition rate of 70 MHz. The synchronization pulse stream transmitted along two paths. Each of the 10 optical signals was passed through a passive optical delay line, each line longer than the previous one by a constant increment. The ten signals were then combined to form the multiplexed output. Comparisons between optoelectronic and optical multiplexing are made and experimental results are presented.

Two novel concepts are examined. First, the use of switched photodetectors for demultiplexing signals in the Gb/s range is investigated. Each channel on a multiplexed data stream is assigned specific time slots. Demultiplexing is achieved by switching a photodetector on during the time slots pertaining to one specific channel. The photodetector is switched on using an electrical gating pulse. This concept has been experimentally demonstrated with two channels at a line rate equivalent to 560 Mb/s and a BER of 10^{-8} has been achieved. Second, the concept of coincidence gates for demultiplexing signals in the Gb/s range is investigated. The idea consists of extracting the gating pulse from the multiplexed signal using delay lines and an optoelectronic AND gate. This technique eliminates the clock recovery circuit found in conventional demultiplexers. Experimental results are presented and some alternative methods for coincidence gating are examined.

REMERCIEMENTS

Je remercie le Docteur R.I. MacDonald et George Fraser qui m'ont procuré l'idée sur lequel cette thèse est basée et les Docteurs G.D. Cormack et R.I. MacDonald pour leur supervision et patience au cours de ces deux dernières années.

Je désire souligner la contribution des Docteurs C.G. Englefield et A.E. Kamal qui ont pris le temps de lire cette thèse et de suggérer des améliorations.

Cette thèse ne serait ce qu'elle est sans la patience infinie et le soutien technique de George Fraser, Darrell Barabash, Graham McKinnon, et Peter Choy. Leur contribution à la partie expérimental du projet de recherche est immense. Je suis très reconnaissant envers Darrell Barabash qui a partagé généreusement et avec patience ses connaissances.

Je remercie le "Alberta Telecommunications Research Centre" et le Docteur R.I. MacDonald pour leur excellent soutien financier et pour m'avoir procuré un environnement idéal pour exécuter mon projet de recherche. L'enthousiasme des membres du ATRC, particulièrement Teresa Lieber, a été une source constante d'inspiration .

Finalement, je remercie du fond du coeur mes parents, Léandre et Maude, et mon amie, Kerry Peterkin, pour avoir cru en moi et pour avoir prêter une oreille attentive lorsque la lumière vascillait nerveusement tout au fond du tunnel des émotions.

TABLE OF CONTENTS

CHAPTER PAGE

1. INTRODUCTION 1

1.1 Multiplexing for high bit rate systems 1

1.1.1 OTDM versus ETDM 2

1.2 Optical Time-Division Multiplexing 5

1.3 Optical Time-Division Demultiplexing 8

1.3.1 Optical switches for demultiplexing 8

1.3.2 Timing of the demultiplexer switches 12

1.3.3 Limitations of demultiplexing with optical switches 12

1.4 Organization of thesis 12

2. OPTOELECTRONIC MULTIPLEXING 14

2.1 Description of an optoelectronic multiplexer 14

2.1.1 Sampling the NRZ electrical data 14

2.1.1.1 Practical consideration for sampling 17

2.1.2 Timing and combining 18

2.2 Multiplexer design requirements 19

2.2.1 Power budget 19

2.2.2 Calculation of required power to obtain a 10^{-9} BER 20

2.2.3 Choice of laser 23

2.2.4 Calculation of a UOD 23

2.3 Electronics for the Multiplexer 24

2.3.1 Laser modulator 25

2.3.1.1 Generating impulses using a SRD 25

2.3.2 Power splitter and phase shifter 28
2.3.3 Shift registers 29
2.3.4 Other modules 30
2.4 Experimental results 30
3. OPTOELECTRONIC DEMULTIPLEXING 35
3.1 Optoelectronic DEMUX 35
3.2 Switched junction photodetectors 37
3.2.1 Switched photodetection for demultiplexing 38
3.2.2 Choice of detector 38
3.2.3 The MSM photodiode 40
3.2.4 Design of MSM 41
3.2.5 Characterization of MSM 44
3.3 Coincidence gating 46
3.3.1 Choice of detector 47
3.3.2 Description of the coincidence gating experiment 47
3.3.3 Discussion of results 51
3.4 Threshold detection as an alternative method for coincidence gating 52
4. DEMULTIPLEXING EXPERIMENT 54
4.1 Multiplexing of two data streams 54
4.2 Demultiplexing 57
4.3 Noise calculation 59
4.4 Experimental results 59
4.4.1 Responsivity under pulsed bias 60
4.4.2 BER measurements 61

5. SUMMARY AND CONCLUSION.....67

REFERENCES.....69

APPENDIX A: EQUIPMENT USED.....72

APPENDIX B: DEVICE DATA SHEETS.....74

APPENDIX C: CIRCUIT SCHEMATICS AND FREQUENCY RESPONSES.....88

LIST OF FIGURES

FIGURE		PAGE
1.1	(a) Electronic time-division multiplexed lightwave system. (b) Optical time-division multiplexed lightwave system.	4
1.2	Modulation with an optical switch	5
1.3	Relative timing of n multiplexed channels	7
1.4	(a) Optical switch block diagram. (b) Simplified switching function	10
1.5	Timing scheme for demultiplexing with a one by two switch [8]	11
2.1	Optoelectronic multiplexer	14
2.2	Sampling electrical NRZ data using the laser threshold characteristic	16
2.3	Clock splitting and pulse generation.	18
2.4	Power losses in the optoelectronic TDM system.	19
2.5	(a) Typical receiver for a lightwave system (b) Eye diagram of the received data	21

2.6 Output of the laser modulator 22

2.7 Multiplexer block diagram 24

2.8 Laser modulator circuit schematic 26

2.9 (a) Laser modulator equivalent circuit.
(b) with the SRD equivalent model 27

2.10 (a) Sinusoidal input.
(b) output at Rl 28

2.11 Power splitter and phase shifter functional diagram 29

2.12 Shift register module functional diagram. 30

2.13 Optoelectronic Multiplexer. 31

2.14 Set-up used to characterize the laser modulator output 32

2.15 Eye diagram of laser modulator number six 32

2.16 Multiplexed signal 33

3.1 Optoelectronic DEMUX 36

3.2 (a) Demultiplexing using switched photodetectors.

(b) Relative timing of the data signals and gating pulses.....39

3.3 MSM cross sectional view.....41

3.4 (a) MSM interdigitated stucture

(b) Array of 8 MSMs.....43

3.5 MSM frequency response measurement.....44

3.6 MSM frequency response.....45

3.7 Optoelectronic AND gate.....48

3.8 Test jig and micro-manipulators.....49

3.9 AND gate experiment.....49

3.10 Output from fibre F1.....50

3.11 Output from fibre F2.....50

3.12 Inputs and EXPECTED output of the optoelectronic AND gate.....51

3.13 Optoelectronic AND gate output.....52

3.14 Data interference on the gating pulse signal.....53

4.1 Transmission experiment.....54

4.2.1 Output from fibre 3.....56

4.2.2 Output from fibre 4.....56

4.3 Relative timing of data signal and gating pulse 57

4.4 Effect of the leakage pulse on the data.....58

4.5 Data amplifier stages 58

4.6.1 Demultiplexing by switched photodetection.....60

4.6.2 Eye diagram of demultiplexed data.....60

4.7 Effect of one additional channel on the BER for Channel 1.....64

4.8 Effect of one additional channel on the BER for Channel 2.....65

4.9 Channel 1 with two active channels.....66

B.1 PIN detector frequency response, Rl = 50 ohms.....87

C.1 Shift register module.....89

C.2 Power splitter / phase shifter.....90

C.3 ECL to TTL converter 91

C.4 Differential amplifier.....92

C.5 Third order Butterworth low pass filter.....92

C.6 Amp. 1 frequency response.....93

C.7 Amp. 3 frequency response.....93

C.8 LPF frequency response.....94

C.9 Differential amp. frequency response.....94

LIST OF ACRONYMS AND ABBREVIATIONS

A	Amperes
BER	Bit Error Rate
cm	Centimeter
CW	Continuous Wave
db	Decibel
dbm	Decibel milliwatt
DC	Constant
DEMUX	Demultiplexer
E/O	Electrical to Optical
ECL	Emitter Coupled Logic
ETDM	Electronic Time Division Multiplexing
Gb/s	Gigabit per second
Gbit/s	Gigabit per second
GHz	Gigahertz
K	Boltzman's constant
KΩ	One thousand ohms
K	Degrees Kelvin
ISI	InterSymbol Interference
LPF	Low Pass Filter
mA	Milliamperes
m/s	Meter per second
MESFET	Type of transistor
Mb/s	Megabit per second
MSM	Metal Semiconductor Metal
MUX	Multiplexer

mV	Millivolts
mW	Milliwatts
NRZ	Non Return to Zero
Ω	Ohm.
nsec	Nanosecond
O/E	Optical to Electrical
OETDM	Optoelectronic Time Division Multiplexing.
OTDM	Optical Time Division Multiplexing
PIN	P-type layer:Intrisic layer:N-type layer.
pf	Picofarad
psec	picosecond
psec	picosecond
RZ	Return to Zero
SRD	Step recovery diode
SNR	Signal to noise ratio
TDM	Time Division Multiplexing
TTL	Transistor Transistor Logic
μA	Microamperes
μm	Micrometer
μW	Microwatt
UOD	Unit Optical Delay
V	Volts
W	Watts

LIST OF SYMBOLS

A_1	Eye opening without ISI.
A_2	Eye opening with ISI.
An	Data channel.
B	Noise bandwidth.
B_-, B_+	Optical switch extinction parameters.
C	Baseband channel rate.
C_{vr}	Junction capacitance.
D	Constant incremental delay.
Dn	Diode n.
E_b	Battery voltage.
E_b'	Equivalent voltage.
E_g	Voltage source.
f_0	Frequency of a damped sinewave.
Fn	Fiber n.
$\langle i^2 \rangle$	Thermal noise current.
I_a	Average current.
I_b	Laser biasing current.
I_{out}	Receiver output current.
I_p	Current pulse amplitude.
I_{pp}	Peak to peak current.
L	Inductance.
n	Donor type.
n	Integer index.
p	Acceptor type.

P_1	Optical switch input power.
P_2	Optical switch output power.
P_3	Optical switch output power.
P_a	Average power.
P_p	Peak power.
Q1	Transistor.
R	Responsivity.
R_l	Load resistor.
Rn	Resistor n.
R_s	Series resistor.
S	Switch.
S	Synchronization pulse.
T	Period of a sinewave.
T	Temperature.
t_d	Time delay.
T_o	Impulse width.
T_{th}	Carrier recombination lifetime at threshold.
V	Optical switch control voltage.
V(-3db)	Voltage at which $P_2 = P_3$.
V_+	Voltage at which the optical switch extinction is minimum.
V_-	Voltage at which the optical switch extinction is maximum.
V_o	Output voltage.
V_p	Impulse height.
W	Width of an optical pulse.

CHAPTER 1

INTRODUCTION

A communication network is often required to carry information from different sources on a single optical waveguide. Combining low bit rate data streams from different sources into a single high speed data stream is called multiplexing. Demultiplexing is of course the reverse operation. There are three commonly used types of multiplexing: Code-division, frequency-division, and time-division. Time-division is the usual method for optical systems. This thesis discusses new technologies for performing optoelectronic time division multiplexing/demultiplexing.

The first part of this chapter discusses Optical Time Division Multiplexing (OTDM)[1] versus Electronic Time Division Multiplexing (ETDM). In the second and third parts optical multiplexing and demultiplexing techniques are discussed and used as examples to present basic concepts. Finally the thesis organization is explained.

1.1 Multiplexing for high bit rate systems

Optical fibre has been recognized as the way to satisfy the need for higher bit rates. Not only does it have a higher capacity per volume of cable than coaxial cable but it is also less lossy, more cost effective, and is not vulnerable to electromagnetic interference.

In recent years the demand for high capacity transmission systems has grown rapidly. As bit rates increase the need for faster demultiplexing becomes obvious. While electronic TDM, using high speed GaAs logic circuits, has so far been adequate it will be increasingly difficult as electronic digital circuits in the 10 Gb/s range are required. At this

[1]Even though the term OTDM literally means multiplexing only, it is used throughout this thesis in the system sense implying both multiplexing and demultiplexing.

high bit rate electromagnetic interference between neighboring electronic devices and connecting lines cause severe difficulties. An alternative to the all-electronic solution is to develop hybrid multiplexers (MUX) and demultiplexers (DEMUX), where the high bit rate signal is processed as optical pulses while demultiplexed low-bit-rate signals are processed electronically [1]. OTDM moves the demand for high speed performance away from the electronics and places it on optical devices. Higher speed is achieved by removing limitations set by the restricted bandwidth of the electronics and by capitalizing on the inherent high-speed characteristics of optical devices.

In OTDM a high bit rate data stream is formed by optically time-multiplexing several lower bit-rate optical streams. At the receiver end of the system the very high bit rate optical signal is demultiplexed to several lower bit rate optical signals by routing the bits to the appropriate detectors using high speed optical switches. The low speed optical signals are subsequently detected and converted to the electrical domain. The OTDM approach is purely digital and therefore agrees well with the trend towards all digital networks and systems. Optical multiplexing and demultiplexing at high bit rates has recently been demonstrated using optical switches. In an experiment by Tucker et al. [2] four channels, each transmitting at 4 Gb/s, were multiplexed and demultiplexed by this method. The aggregate transmission bit rate was 16 Gb/s. The work reported in this thesis uses a novel approach to time division multiplexing and demultiplexing that does not use optical switches.

1.1.1 OTDM versus ETDM

The basic principle of time division multiplexing and demultiplexing is that each baseband channel is allocated a series of time slots on the multiplexed output. The MUX

combines all baseband channels to form the high bit rate multiplexed signal. The DEMUX reconstructs all baseband channels by extracting the bits from the multiplexed data stream.

Fig. 1.1 illustrates the basic differences between electronic and optical time multiplexed lightwave systems. In the electronically multiplexed lightwave system (Fig. 1.1 (a)) multiplexing occurs in the electrical domain before the optical to electrical conversion (O/E). Similarly, demultiplexing is performed electronically after the O/E. Consequently the required bandwidth of the electronics in the MUX, DEMUX, and O/E must be sufficient to pass the composite bit rate of the multiplexed signal nB, where n is the number of channels and B the bit rate of a single channel. The MUX, DEMUX, O/E, and E/O therefore operate at maximum bit rates determined by the speed limitation of digital integrated circuits and the limited bandwidth of high speed laser modulators. So far the performance of electronic MUX and DEMUX units has been limited to about 10 Gb/s [3,4].

In the optically multiplexed system, as shown in Fig.1.1 (b), the bandwidth limitations due to the MUX and DEMUX are removed because multiplexing and demultiplexing occur in the optical domain.

There is an important difference between electronic and optical multiplexing systems. In electronic systems the multiplexing and demultiplexing operations can be carried out at points in the system where the amplitude of the signal is large. As a result, the receiver sensitivity does not need to be increased to make up for the losses in the MUX and DEMUX. The required SNR is determined by the O/E and its associated low noise front end. In OTDM multiplexing and demultiplexing operations are carried out on the optical signal. Thus optical losses reduce the SNR at the receiver and it is important to minimize them. One solution is to use optical amplifiers to compensate for these losses [5].

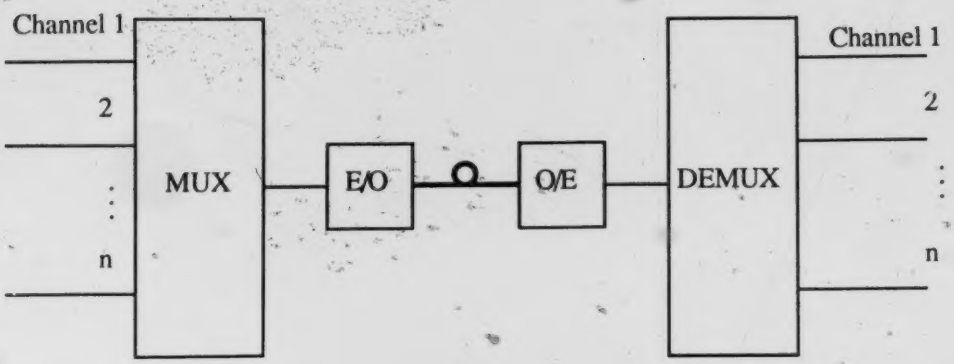

(a)

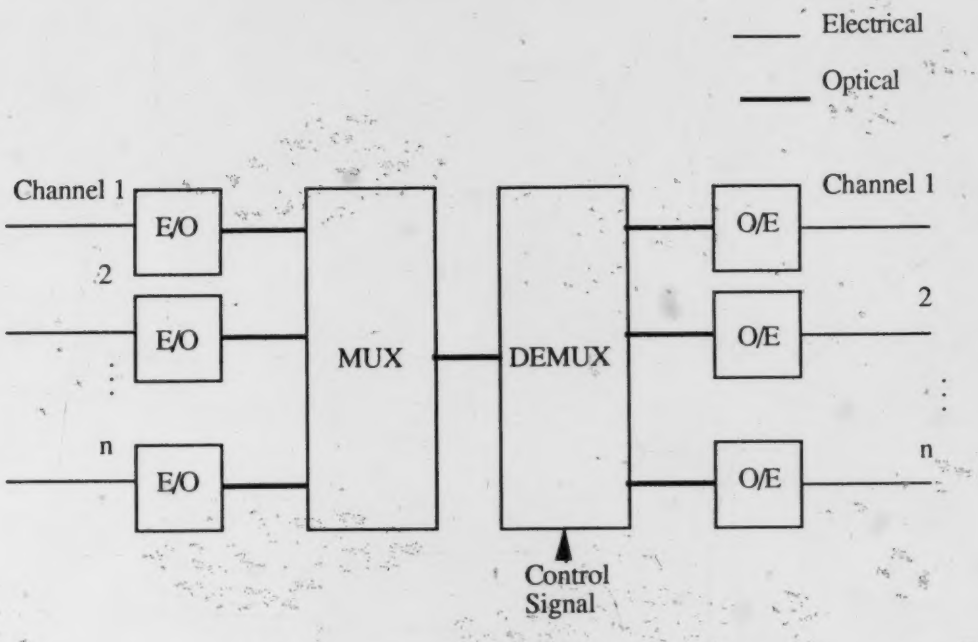

(b)

Fig.1.1 (a) Electronic time-division multiplexed lightwave system.

(b) Optical time-division multiplexed lightwave system.

1.2 Optical Time-Division Multiplexing

Sampling, timing, and combining are the three basic subfunctions of time-division-multiplexing. The sampling function identifies the value of the incoming bit from every baseband channel. Timing ensures that the samples taken are available during their appropriate time slots on the multiplexed data stream. All data streams from the baseband channels are then assembled using the combining function to form the high speed multiplexed data signal.

The sampling function is best realized using optical pulses from mode-locked [6] or gain switched [7] lasers which are capable of generating pulses more than ten times shorter than electrical pulses [8]. Shorter pulses allow for a higher multiplexed data rate. Let us consider the approach where the sampling is carried out in the E/O converter. As shown in Fig.1.2, the short laser pulses sample the electrical data to produce the RZ optical data. The optical modulator can be viewed as an AND gate, meaning that the optical output is the result of ANDing the optical pulse stream and the electrical data.

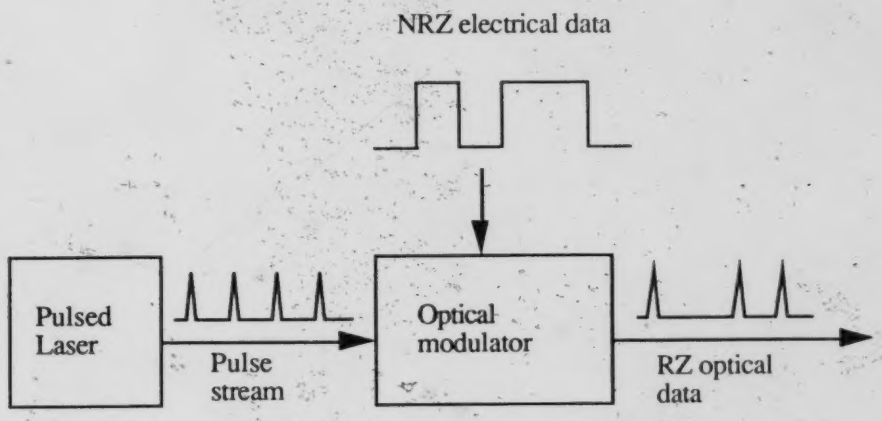

Fig. 1.2 Modulation with an optical switch.

NRZ electrical data, as opposed to RZ, is usually preferable because it minimizes the bandwidth requirement of the baseband digital electronics. Sampling the baseband data in the E/O converter has several advantages. First, the combining function can be carried out passively using a simple star coupler. Second, the RZ nature of the baseband optical data will generate very low multiplexing crosstalk (pulse overlap) when combined to form the multiplexed output. Third, laser output power is used efficiently because the laser is transmitting only during the time slots pertaining to its own channel. This is an important consideration since semiconductor lasers are average-power-limited devices [8].

The timing for the n baseband channels is shown in Fig. 1.3 where there is a constant incremental delay, D, between two consecutive channels. All bits are shown as "ones" for clarity. The delays can be implemented electrically by introducing a phase shift on the clock signal or optically using passive delay lines [9]. If the pulse spacing is adjusted for a maximum bit rate, each pulse in the multiplexed bit stream comes in contact with its nearest neighbors. In this case D=W and the multiplexed bit rate is 1/W. With a pulse width W of 100 psec the maximum achievable multiplexed bit rate is 10 Gb/s. In practice, pulses have leading and trailing tails that will overlap and cause crosstalk if the pulse spacing is insufficient. It is usual practice to ensure that the pulse width is shorter than the multiplexed bit period ($W < D$) so that cross talk is minimized. However, reducing the pulse width increases the frequency content of the pulse stream and causes each pulse to widen due to fibre dispersion. A compromise has to be made between system crosstalk and pulse spreading, the latter being proportional to the fibre length. In a long haul system it might be better to choose a larger pulse width to reduce pulse spreading at the expense of increasing system crosstalk. If transmission is over a short length of fibre, dispersion becomes insignificant. Therefore, a short pulse minimizing system crosstalk may be advantageous.

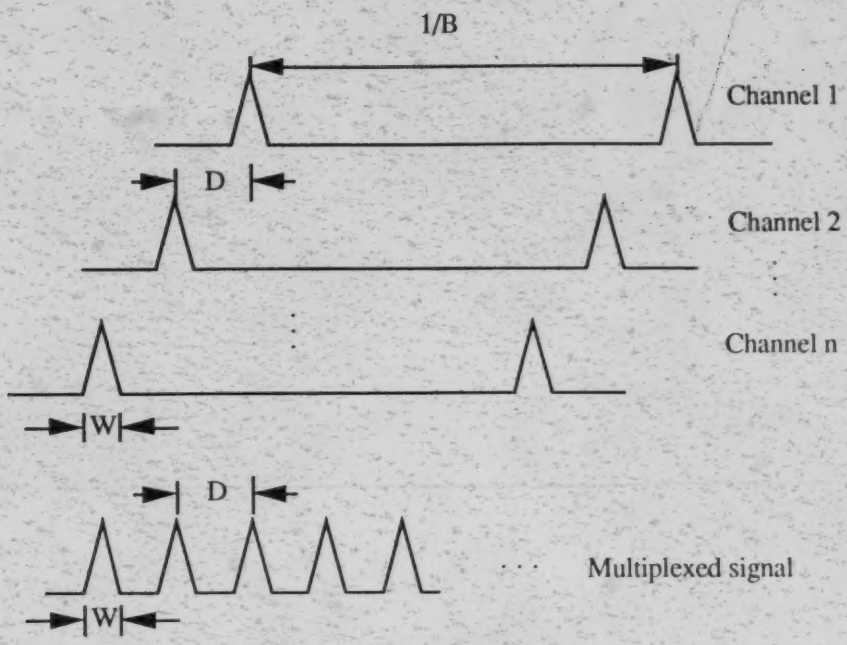

Fig. 1.3 Relative timing of n multiplexed channels.

Combining is the last basic operation of multiplexing and can be achieved either passively or actively. A passive optical combiner uses a device such as a biconical tapered fibre coupler [10] or a star coupler. This approach is simple technologically and cheap compared to active combining. A two by one fibre coupler costs around 200 dollars while the price of an optical switch is several thousand dollars. The main drawback of a passive power combiner with n inputs is that the insertion loss, 10 log (n), can be fairly high. An active combiner, using an optical switch, has the potential to reduce insertion loss significantly since the loss per device is small. However, power loss in a passive combiner can always be compensated for, by using an optical amplifier [5].

An active combiner could reduce pulse overlap due to the leading and trailing tails of the RZ optical pulses. In a passive combiner the pulse tail extends into the neighboring time slot causing crosstalk, which degrades the BER performance of the receiver. In

addition, a Ti:$LiNbO_3$ switch used as an active combiner could, in principle, eliminate the need for pulsed lasers. However, this approach is hardly practical with todays devices because of the very stringent requirements on the on/off extinction ratio and the switching speed of the switch [8]. In addition the above mentioned approach would limit the optical pulse peak power to the maximum CW operation power of the semiconductor laser.

Active combining does not offer significant improvements in performance over passive combining. Consequently the latter is usually the preferred option because of its ease of implementation and lower cost.

1.3 Optical Time-Division Demultiplexing

The demultiplexer is the most critical element of an OTDM system. The demultiplexing operation can be divided into three subfunctions. First, each bit from the incoming multiplexed data stream is directed to its appropriate channel. Second, the bit is sampled and finally a decision is made to determine whether it is a "zero" or a "one". The last operation is purely electrical and will not be discussed here.

1.3.1 Optical switches for demultiplexing

When optical switches are used for demultiplexing the operation of directing and sampling the bits are combined into one. The optical switch transfers the entire bit to the appropriate channel. Switching the entire bit rather than just sampling it increases the average power received per bit period and therefore eases receiver sensitivity requirements. When switching the entire bit, one has to be careful not to switch the data from the neighboring time slot. Having part of a bit directed to the wrong channel is a source of crosstalk.

The basic block of the demultiplexer is a one by two switch. One switch is sufficient to implement a demultiplexer with two channels. Fig. 1.4 shows the block diagram of the switch and its associated simplified switching function. The switching characteristics can be written as:

$$P_2 = P_1 f(V).$$

$$P_3 = P_1[1-f(V)].$$

Note that the switch is an analog device and that its extinction is not perfect. Even at V_- and V_+, P_2 and P_3 have minimum output power given by the extinction coefficient B_- and B_+ respectively. One can also see that there is a significant power at both outputs over an important range of the control voltage (between V_- and V_+). The extinction ratio, the switching function waveform, and the pulsewidth all affect the crosstalk in the system. The effect of the extinction ratio on the crosstalk is shown in Fig. 1.5 where all bits are shown as "ones" for purpose of clarity. The first waveform is the multiplexed data stream at the input of the switch, which is used here as a two channel demultiplexer. The switch is driven by a square wave with a frequency of half the input bit rate as shown in Fig. 1.5 (2). The next waveform shows the output characteristic of the switch when driven by the square wave (2). The last two waveforms show the outputs P_2 and P_3, where crosstalk resulting from the limited extinction of the switch is illustrated as small unwanted pulses between the main pulses.

The switching function waveform and the pulsewidth affect the crosstalk that occurs while the switch is in transition from one state to another. This type of crosstalk occurs because the receiver integrates all photoelectrons detected in a multiplexed bit period including those which were generated while the switch was changing state.

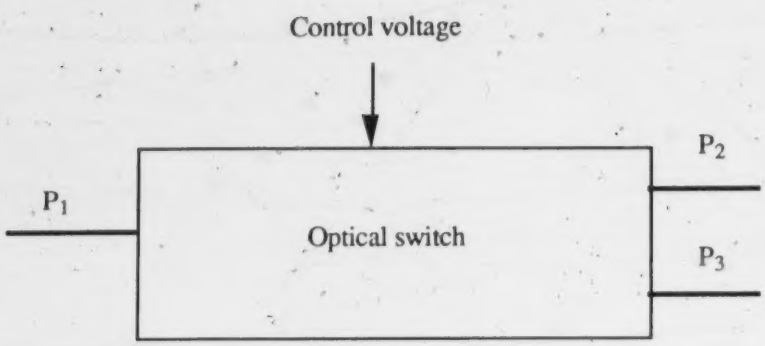

(a)

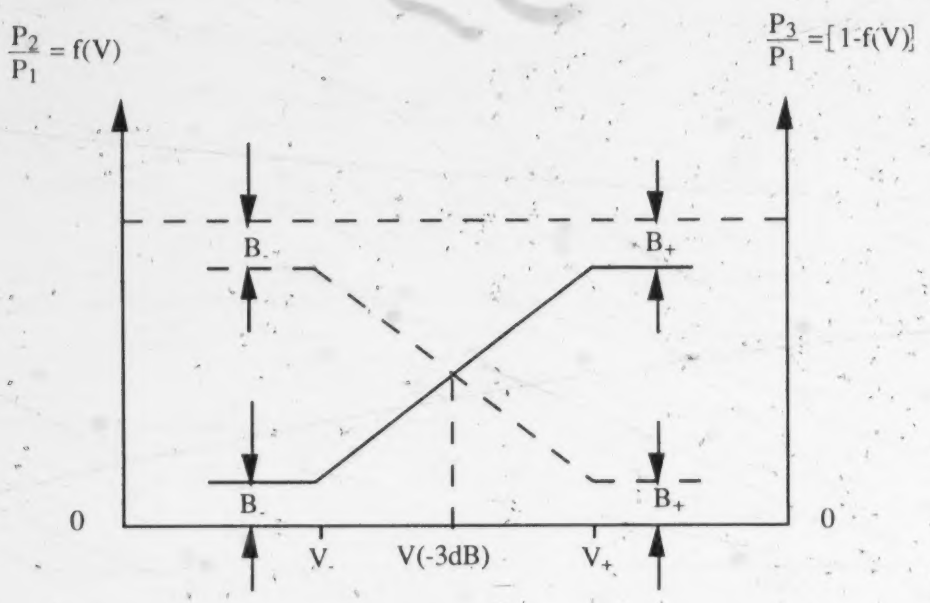

(b)

Fig: 1.4 (a) Optical switch block diagram.

(b) Simplified switching function.

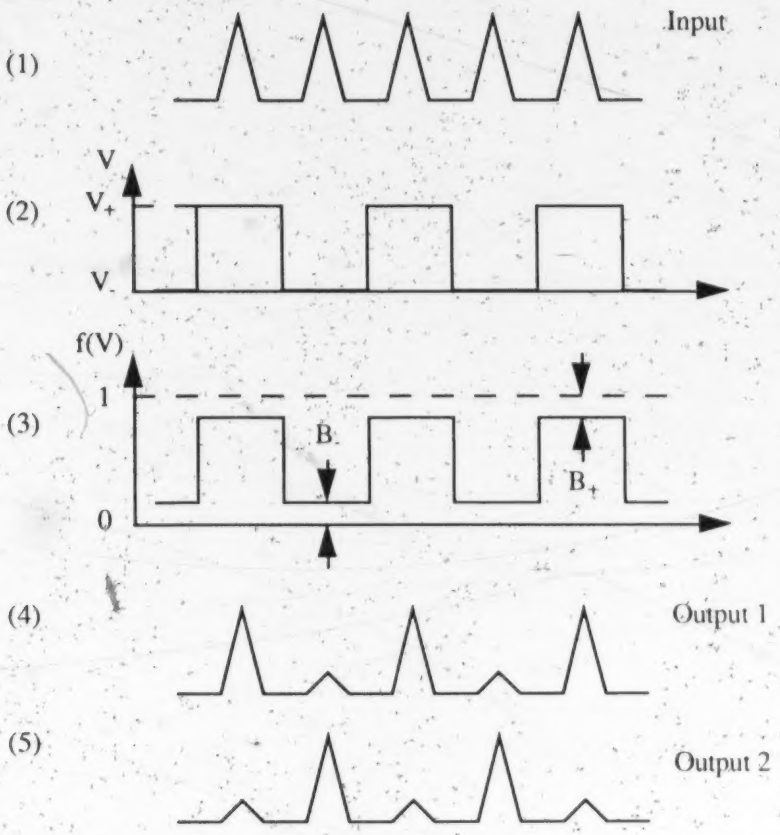

Fig. 1.5 Timing scheme for demultiplexing with a one by two switch [8]

When discussing the effect of the finite extinction of the switch on the crosstalk it was assumed that the control voltage was a square wave. In practice it is extremely difficult to generate a square wave in the GHz frequency range to drive the switch because of the wideband electronics involved. The option is to use a sinusoidal wave at half the frequency of the bit rate to approximate the square wave. A sinusoidal waveform, even at several GHz, is relatively easy to generate since it only requires narrowband electronics. The effect of using a sinusoid as the control voltage, instead of a square wave, is to increase the transition time of the switch. With a longer transition time more photoelectrons from neighboring bits are integrated and the crosstalk becomes higher.

1.3.2 Timing of the demultiplexer switches

Correct timing of the switch is critical if successful demultiplexing is to be achieved. Since there is no electrical signal at the multiplexed bit rate available at the receiver, the clock has to be recovered from the baseband data stream. This is achieved by using the data stream to drive a microwave phase-locked loop. The sinusoidal output of the phase-locked loop becomes the control voltage of the switch.

1.3.3 Limitations of demultiplexing with optical switches

Crosstalk is the main limitation of demultiplexing using optical switches. Crosstalk has two main sources. First, finite extinction of the switch causes part of the neighboring channel to couple through the switch in the off state. Second, the switch sinusoidal control voltage and switching function causes photoelectrons from adjacent bits to be collected with the demultiplexed data stream. Other important problems arise when a multi-channel demultiplexer is built. For a demultiplexer with n output baseband channels, (n-1) switches are assembled in a binary tree or linear configuration. The more switches there are the more difficult it is to synchronize them all especially at Gb/s rates. Each additional switch introduces excess loss which reduces the sensitivity of the demultiplexer. For a system with four channels the insertion loss is around 12 dB [8].

1.4 Organization of thesis

The following chapters present novel optoelectronic techniques for MUX/DEMUX and compare them with the OTDM system described in this chapter.

The construction of an optoelectronic multiplexer using passive optical delay lines and a power combiner as a mean of multiplexing is described in Chapter 2. Eight channels,

each transmitting at 70 Mb/s are multiplexed to form a combined bit rate of 560 Mb/s. Experimental results are presented.

Chapter 3 presents a novel optoelectronic demultiplexing scheme. First, the use of switched photodetectors for demultiplexing is investigated. Second, coincidence gating performed with PIN diodes is discussed and experimental results are presented.

Chapter 4 presents an experiment where switched photodetectors are used to demultiplex the equivalent of a 560 Mb/s signal. Experimental results are presented and discussed.

Chapter 5 summarizes the advantages and disadvantages of optoelectronic TDM systems and presents some interesting future prospects for this technique.

CHAPTER 2

OPTOELECTRONIC MULTIPLEXING

In general "optoelectronic" implies that there is conversion from light to electricity or vice versa. Optoelectronic multiplexing means that one or more of the multiplexing subfunctions (sampling, timing, combining) is carried out by an optoelectronic device. In the multiplexer presented in this chapter the sampling function is carried out by an optoelectronic device, namely, the laser. Optoelectronic multiplexing tries to capitalize on well developed electronic techniques and on promising avenues offered by optical technology such as increased transmission bandwidth.

This chapter contains three sections. First, the concept of the optoelectronic multiplexer is explained. Second, the construction of a multiplexer transmitting at a line rate of 560 Mb/s is described. Finally, experimental results are presented.

2.1 Description of an optoelectronic multiplexer

The optoelectronic multiplexer is shown conceptually in Fig. 2.1. There are eight data channels (A0-A7) and two synchronization channels. The bottom laser generates a synchronization pulse which is split into two paths prior to a differential delay and subsequent combining. The total number of channels being multiplexed is 10.

2.1.1 Sampling the NRZ electrical data

Low duty cycle RZ optical data are required to form the high bit rate multiplexed data stream. The NRZ electrical data of the baseband channels must therefore be sampled in order to obtain the low duty cycle RZ format. The threshold characteristic of the light curve of a semiconductor laser presents a convenient way to sample the data as shown in Fig. 2.2.

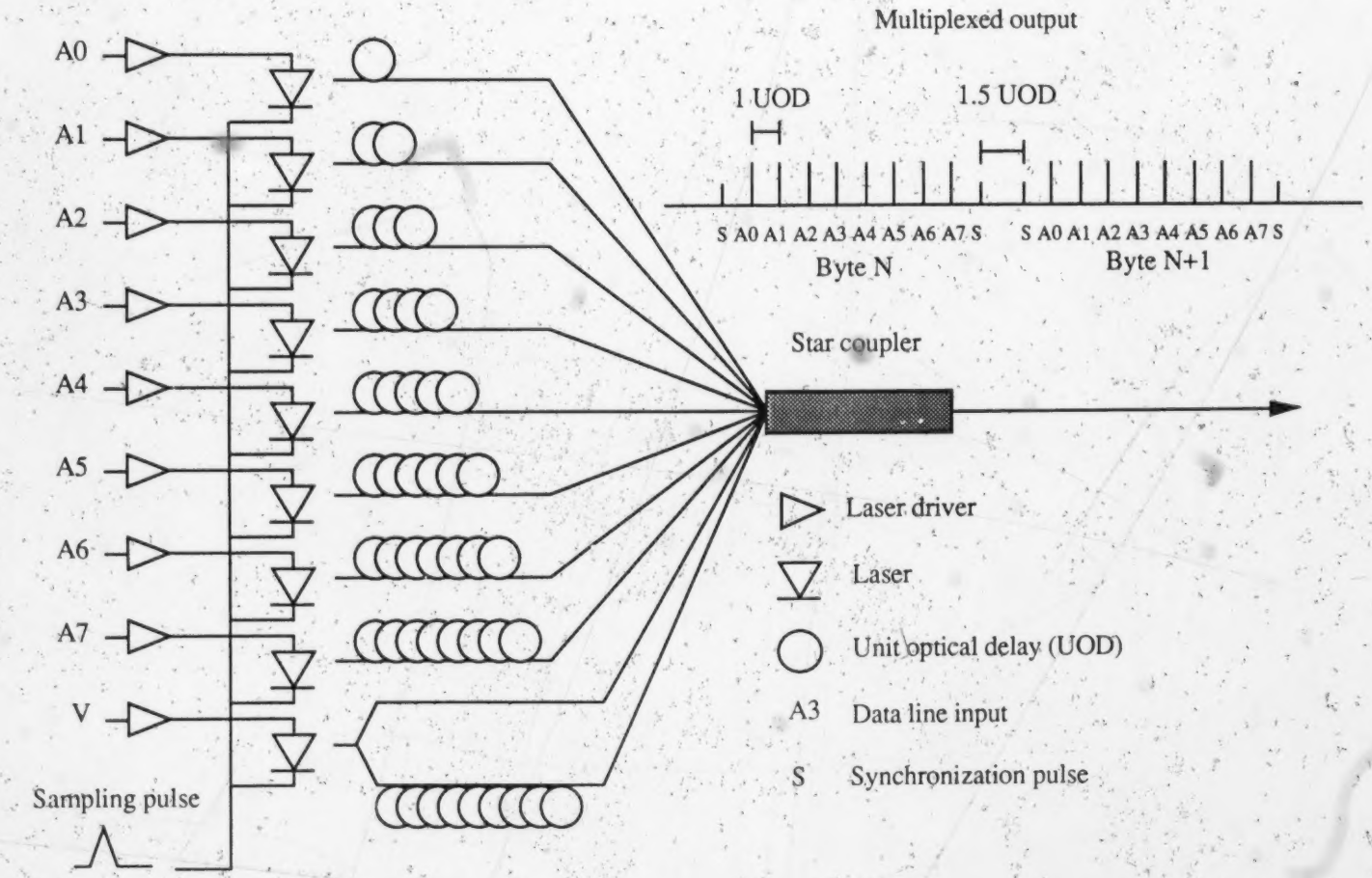

Fig. 2.1 Optoelectronic multiplexer

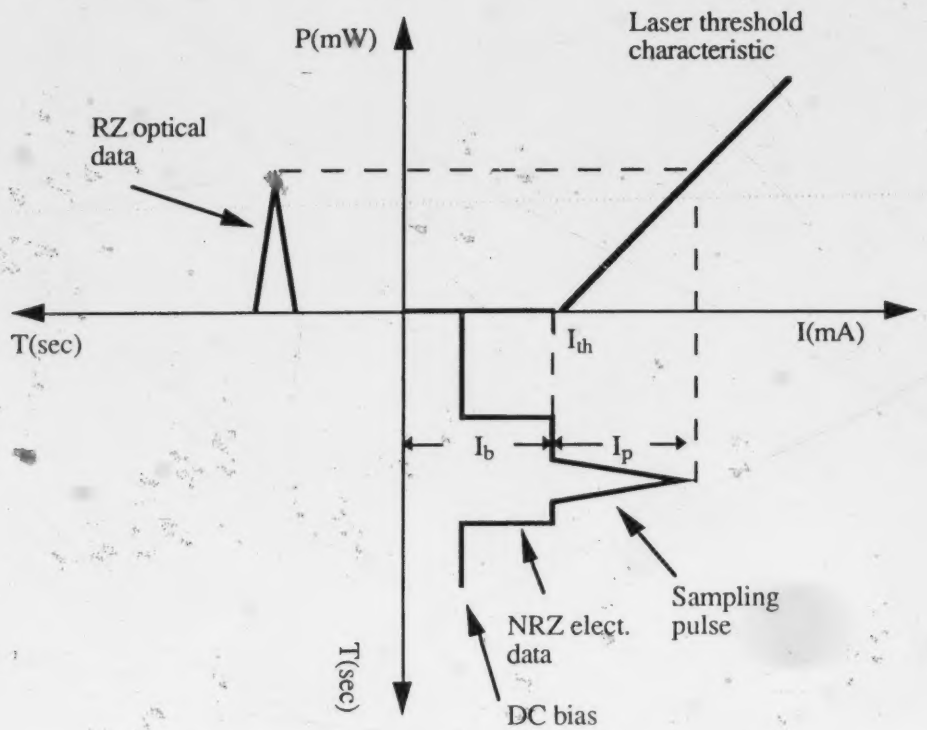

Fig. 2.2 Sampling electrical NRZ data using the laser threshold characteristic.

The "one" symbol in the NRZ data stream and the DC bias set the laser current to just below its threshold value. The sampling pulse increases the laser current to well above its threshold value causing the laser to generate the RZ optical data steam. This technique is called "laser strobing" in this thesis.

Although very simple, this method has drawbacks. Any amplitude variation of the NRZ electrical data directly affects the amplitude of the optical output. Furthermore, when a laser is turned on with a current pulse I_p, a delay t_d, [11] in the emission of light is observed, equal to

$$t_d = T_{th} \ln (I_p/(I_p - I_{th})), \tag{2.1}$$

where T_{th} is the carrier recombination lifetime at threshold (usually about 2 nsec). If the laser is DC-biased with a current I_b, however, (2.1) becomes

$$t_d = T_{th} \ln(I_p/(I_p+I_b-I_{th})), \tag{2.2}$$

and the delay is seen to vanish when $I_b = I_{th}$. Any variation in the level of the NRZ data or DC bias changes the turn-on delay of the laser. This means that the elapsed time between consecutive bits will be slightly different. This phenomenon, called timing jitter, results in substantial problems with receiver design because there is uncertainty as to when the incoming bit will occur.

One noteworthy point about laser strobing is that the laser is used very efficiently since it emits light only when a "one" is transmitted. This is an important practical consideration since semiconductor lasers are average-power-limited devices.

2.1.1.1 Practical consideration for sampling

A sampling pulse of a few volts amplitude and a full width of less than one nsec will be required to achieve gigabit multiplexing with high optical power from the laser. Consequently the sampling pulse prior to splitting must have an amplitude of 10 volts or more. Producing pulses with large amplitude and narrow width requires a very careful design. The solution chosen, as shown on Fig. 2.3, is to split the clock signal, and then to generate the high speed pulses using step recovery diodes [12]. It is also easier to split a sinusoidal clock signal compared to a high speed pulse train. The difficulties in splitting a high speed pulse train are due to the large number of harmonics that are present.

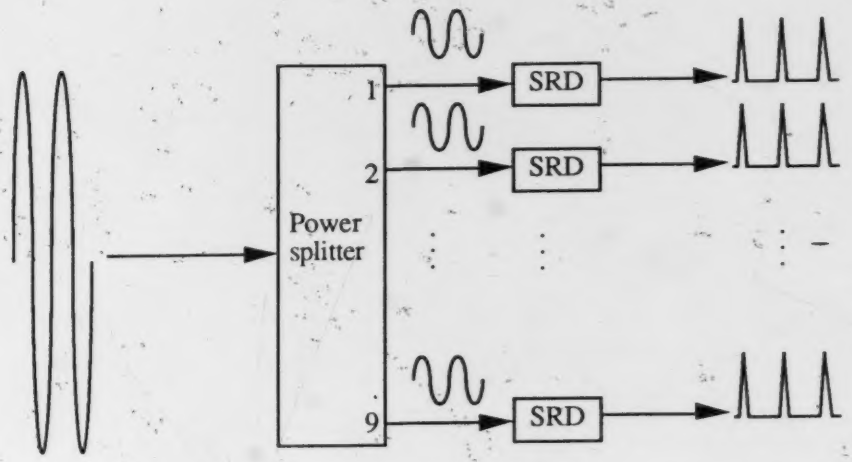

Fig. 2.3 Clock splitting and pulse generation.

2.1.2 Timing and combining

For the last two multiplexing subfunctions, timing and combining, an optoelectronic MUX uses delay lines and passive power combiners. The timing of data and synchronization pulses is realized using passive optical delay lines. Each of the optical bit streams is passed through an optical delay line, each line having a delay that is longer than the previous one by a constant increment called a Unit Optical Delay (UOD). As shown in Fig. 2.1, the time between each pulse within a byte is one UOD. All bits in this figure are represented as "ones" with no time dimension for purpose of clarity. It is clear that the pulse width must be less than one UOD otherwise pulse overlapping will occur. One synchronization pulse is positioned at the beginning of the byte, the other at the end of it. The elapsed time between two consecutive bytes is 1.5 UOD and the reason for this will become clear when the demultiplexer is described. The combining function is realized passively using a 10 x 10 star coupler.

2.2 Multiplexer design requirements

In this section the peak power required per laser modulator is calculated based on a required BER of 10^{-9} at the demultiplexer. A laser is chosen based on these findings. Finally, the value of a UOD is calculated.

2.2.1 Power budget

Fig. 2.4 shows where the power losses occur in the system. Lasers used for transmission systems usually come in a package with an output fibre already coupled to the laser chip. This fibre is called the pigtail and the entire unit is called a pigtailed laser. It is convenient to consider the pigtailed laser as a single device with the output power measured at the end of the pigtail rather than at the laser chip facet. The coupling loss due to pigtailing, approximately 4 dB, will therefore not be accounted for in the power budget.

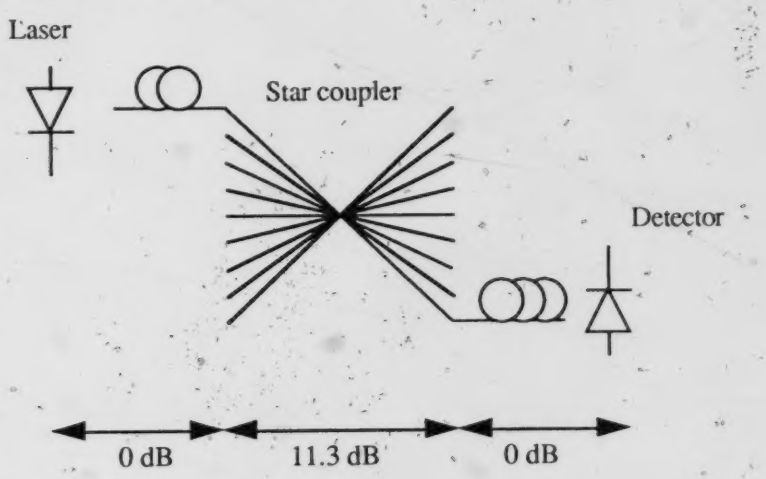

Fig. 2.4 Power losses in the optoelectronic TDM system.

The losses due to the fusion splices are negligible. The loss from the star coupler averages 11.3 dB. There is only a very small coupling loss between the output fibre and

the detector because the detector active area is about four times as large as the radiation pattern of the light from the fibre. The total loss is therefore 11.3 dB.

2.2.2 Calculation of required power to obtain a 10^{-9} BER

A typical receiver is shown in Fig. 2.5 (a). If it is assumed that the dominant source of noise at the receiver is the 25 ohm load then the total receiver noise is the thermal noise current :

$$\langle i^2 \rangle = 4KTB/R, \tag{2.3}$$

where B is the noise bandwidth of a 70 MHz third order low pass filter and equal to 100 MHz, T is the room temperature in degrees Kelvin assumed to be 300 degrees, and K the Boltzman's constant . Substituting these values in (2.3) yields

$$\langle i^2 \rangle = (4 \times 1.38\text{E-}23 \times 300\ \text{K} \times 100\ \text{MHz}) / 25\ \text{ohms} = 6.62\text{E-}14\ \text{A}^2.$$

For a BER of 10^{-9} the ratio of the peak-to-peak signal current (I_{pp}) of the received data, to the RMS noise current, $\sqrt{\langle i^2 \rangle}$, is 21.6 dB [22]. I_{pp} is given by

$$\sqrt{\langle i^2 \rangle\ \text{SNR}}, \tag{2.4}$$

$$= \sqrt{6.62\text{E-}14\ \text{A}^2 \times 144} = 3.09\ \mu\text{A}.$$

The eye diagram of a 70 Mb/s data signal received with a receiver such as that of Fig. 2.5 (a) is shown in Fig. 2.5 (b). The data current, I_{out}, only has positive values due to the inherent unipolar nature of optical signals and to the positive bias on the detector. The average value ,I_a, of such a signal is calculated graphically to be approximately half the peak to peak value, I_{pp}. This yields $I_a = 1.54\ \mu A$. This figure is also the current flowing out of the detector assuming that the pre. amp. and post amp. have a zero dB amplification for the purpose of this calculation.

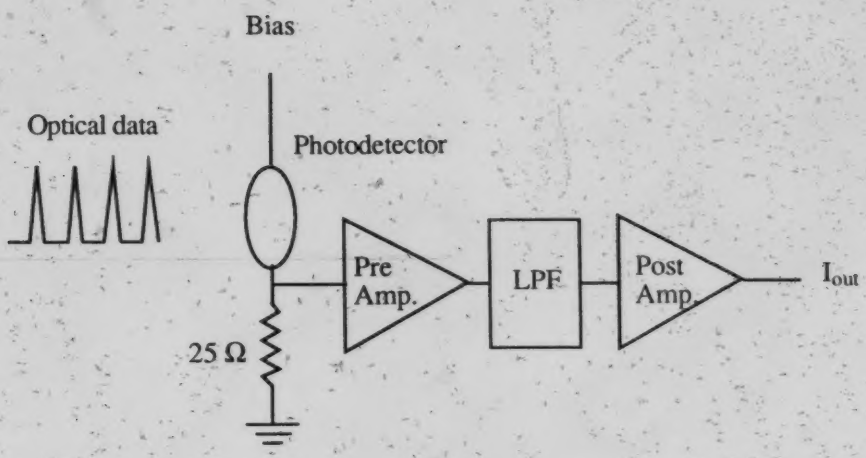

(a)

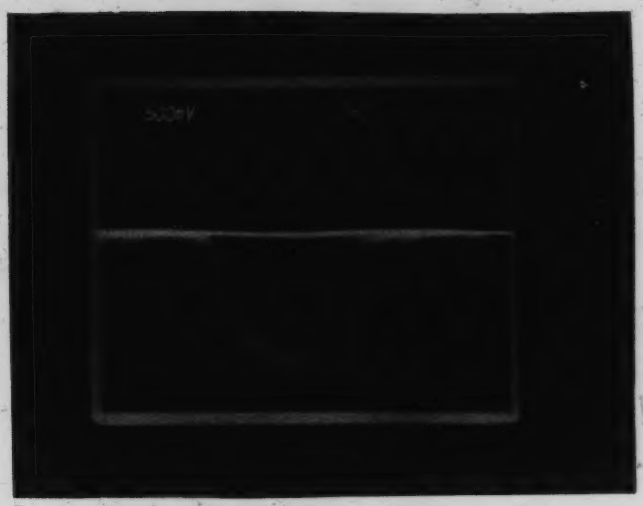

(b)

Fig. 2.5 (a) Typical receiver for a lightwave system and

(b) Eye diagram of the received data

The responsivity of a photodetector is the ratio of the detector output current to the optical power received. Assuming a responsivity, R, of 0.16 A/W for the detector, the average power received per detector, P_a, is

I_a / R (2.5)

$= 9.65\ \mu W.$

The average power coming out of the laser has to be 11.3 dB higher than 9.65 μW to compensate for the loss in the star coupler. The average power required from the laser is thus 130 μW.

What is measured at the laser output is the peak power of the data pulse. Consequently, it is required to convert the average power into a peak power. Fig. 2.6 shows the data pulse at the output of the laser.

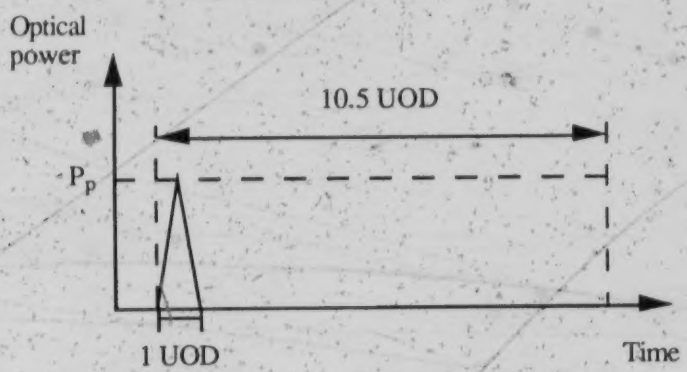

Fig. 2.6 Output of the laser modulator

One data pulse occupies 1 UOD out of the 10.5 UODs taken by one byte. The data pulse is assumed to be triangular and its average power (P_a) over a time period of 10.5 UODs is the energy of the pulse,

$(P_p \times 1\ UOD) / 2,$

divided by the duration of a byte, 10.5 UODs, which yields

$P_a = P_p / 21.$ (2.6)

The peak power required to obtain a BER of 10^{-9}, P_p, becomes 2.7 mW.

2.2.3 Choice of laser

It was imperative to limit the cost of each laser to a few hundred dollars since nine were required for the multiplexer. Also the bandwidth of the laser must be sufficient to allow for transmission at a bit rate of several hundreds Mb/s. The third requirement on the laser was that it must produce an output peak power of at least 2.7 mW. The laser chosen was the ML6411C from Mitsubishi for which, the data sheets are as in Appendix B. It was commercially packaged and pigtailed. The pigtailed laser has a maximum output peak power of approximately 10 mW. Tests were performed and it was found that pulses with a peak power of approximately four mW and a full width of about 1.4 nsec could be obtained by pulsing the injection current of this laser. The wavelength was 780 nm and each unit cost $ 350.

2.2.4 Calculation of a UOD

As shown in Fig. 2.1, one byte is 10.5 UOD long. Because the baseband channel rate, C, was chosen to be 70 Mb/s, the length of a byte must be equal to 1/C or 14.3 nsec. The value of one UOD is

14.3 nsec / 10.5 = 1.36 nsec.

The speed of light inside a given material is inversely proportional to its index of refraction. The fibre core index of refraction is 1.47, so the speed of light inside the fibre core is 2.04E8 m/s. The length of fibre required for a UOD is therefore2.04E8 m/s x 1.36 nsec = 27.7 cm.

The multiplexed bit rate will be the number of channels times the channel rate:

8 x 70 Mb/s = 560 Mb/s.

2.3 Electronics for the Multiplexer

The electronics for the multiplexer consisted of the modules shown in Fig. 2.7.

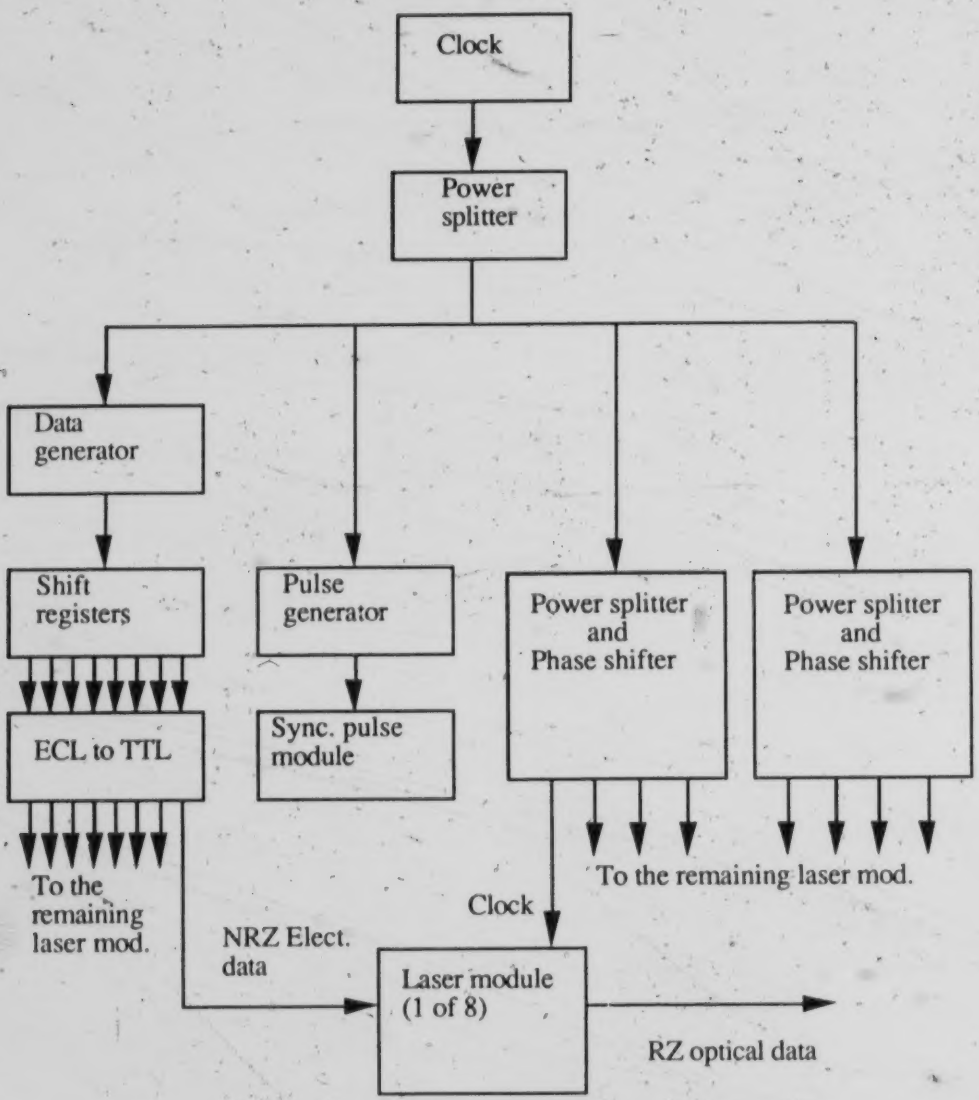

Fig. 2.7 Multiplexer block diagram.

With the exception of the clock, the data generator, the power splitter, and the pulse generator all the modules had to be designed and built. The purpose and design of the modules that were built are explained in the following sections.

2.3.1 Laser modulator

The laser modulator must produce RZ data with a 1.36 nsec duration and a peak power of about 2.7 mW. As shown in Fig. 2.8, the inputs to the laser modulator consist of the clock and data signals. This circuit can be considered as two subcircuits. The first subcircuit consists of the voltage regulator LM317 and all the components connected to it . Its purpose is to provide a stable bias current for the laser through resistor R6.

The second subcircuit, explained in the next section, is everything to the left of resistor R4. Its purpose is to convert the sinusoidal clock into a train of narrow unidirectional impulses using a step recovery diode (SRD). The SRD used in this circuit is the Alpha DVB6100B. Current from the pulse stream flows through R4 and is added to the DC current and the current generated by the data at the node common to R4, R5, R6, and the laser diode D2. The combined current flows in the laser diode.

2.3.1.1 Generating impulses using a SRD

Fig. 2.9 (a) shows a simplified circuit of the laser modulator. Everything to the right of the SRD was replaced by an impedance of arbitrary value R_l. The sinusoidal signal generator, the inductance, and the battery replace transistor Q1. In Fig. 2.9 (b) the SRD is replaced by its equivalent model.

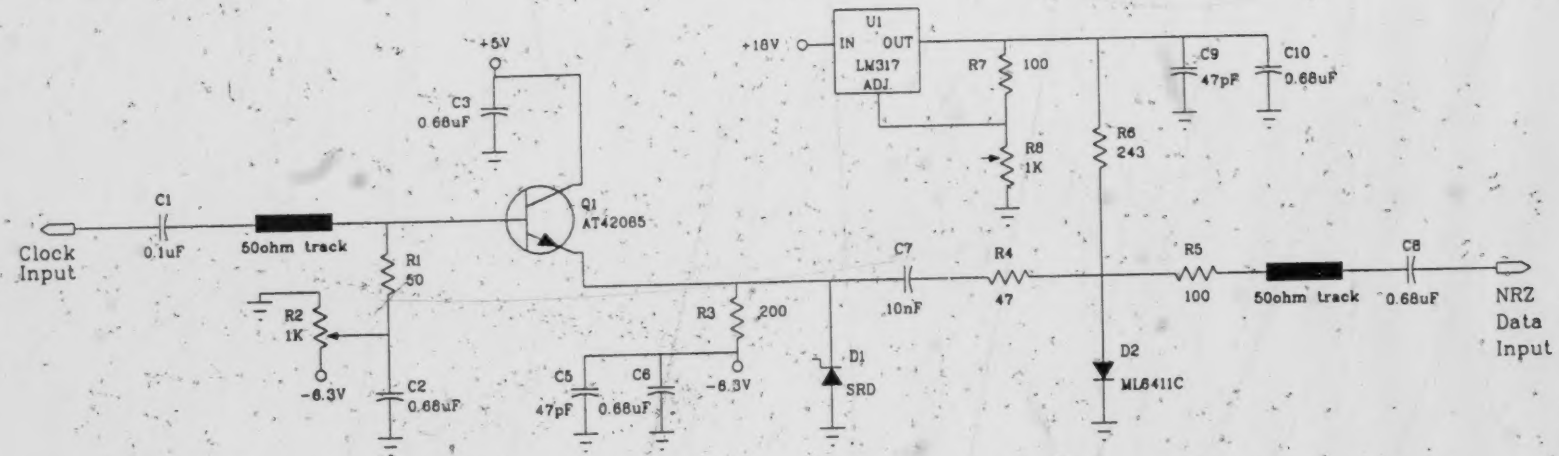

Fig. 2.8 Laser modulator circuit schematic

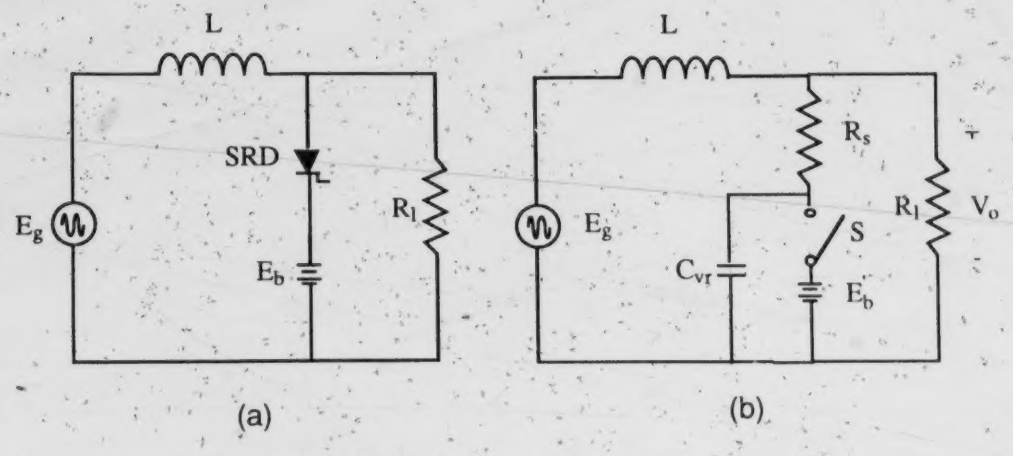

Fig. 2.9 (a) Laser modulator equivalent circuit and
(b) with the SRD equivalent model.

A step recovery diode can be best described as a charge controlled switch. When charge is inserted into the diode by a forward bias voltage, the switch is closed and the SRD appears as a very small resistor R_s which is equivalent to a short circuit. If the charge is removed by reversing the bias on the SRD the switch remains closed until all the charge is removed. At this point the switch opens rapidly and the diode becomes equivalent to a small capacitance, C_{vr}.

Before the signal generator is turned on and during the positive half cycle of the sinusoid the switch in the equivalent model is closed and the SRD appears as a short, letting no current go through R_l. In the negative half cycle the charge is removed. When the charge is completely removed, the switch opens and the SRD appears as a very high impedance (small capacitance C_{vr}). The rapid cessation of the SRD current creates a transient waveform involving L, C_{vr}, and R_l. If $R_l > \sqrt{\frac{L}{C_{vr}}}$, the transient takes the form of a damped high frequency sinewave of frequency [13]

$$f_o = \frac{1}{2\pi\sqrt{LC_{vr}}}$$

The first half of the transient forms the output pulse. When the negative half of the transient occurs the diode becomes forward biased again and shorts R_l. The current in R_l is a series of unidirectional impulses with a repetition rate at precisely the frequency of the input sinusoid as shown in Fig. 2.10. The impulse width, T_o, is

$\pi\sqrt{LC_{vr}}$ and

the impulse height, V_p, is [13]

$E_b'T\pi / (2T_o)$.

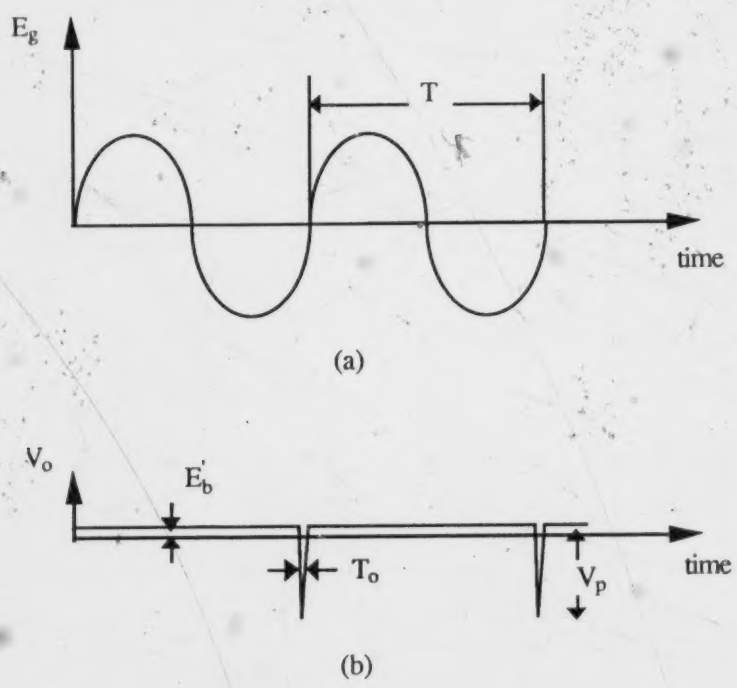

Fig. 2.10 (a) Sinusoidal input and,

(b) output at R_l.

2.3.2 Power splitter and phase shifter

This circuit performs two distinct operations on the incoming clock signal. First as shown in Fig. 2.11, it splits the clock into four signals of equal amplitude. The power

splitters used were the PSC-4 from Mini-Circuit. Its excess loss is in the order of 1 dB. The second operation is to provide independent variable delays for the four resulting clock signals. The purpose of the variable delays is not to replace the passive optical delays but to provide a means to compensate for any phase differences between the laser modulators. The phase differences are caused by several factors, notably the differences in SRD characteristics and the variation of SRD biases, E_b. The type of delay used was a Tee-section and the delay obtained varied from zero to eight degrees (or zero to 0.4 nsec) with an amplitude variation of about one percent over this range. The circuit schematic is provided in Appendix C.

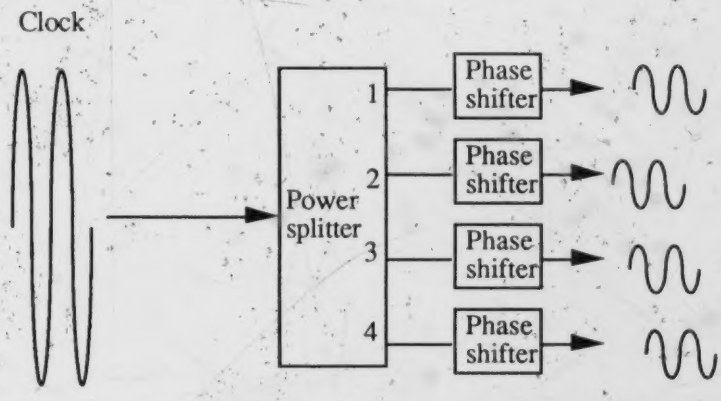

Fig. 2.11 Power splitter and phase shifter functional diagram.

2.3.3 Shift registers

For reasons of economy it was not possible to purchase eight different data generators to drive every laser modulator with a different bit stream. One data generator drives a circuit made up of 32 one-bit shift registers connected in series as shown in Fig. 2.12. The circuit is tapped at every four shift registers to provide a data stream delayed by four bits compared to the previous output. There are eight outputs (A0-A7); the minimum

incremental delay between two data streams is four bits and the maximum 28. The circuit uses ECL technology and its schematic is shown in Appendix C.

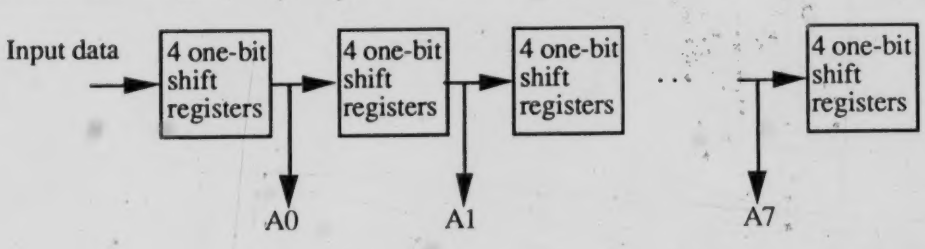

Fig. 2.12 Shift register module functional diagram.

2.3.4 Other modules

The purpose of the modules in Fig. 2.7 that have not been described so far is explained briefly in this section. The purpose of the synchronization module is to generate the optical synchronization pulse. The circuit consists of a laser diode with a biasing network. The electrical pulse necessary to drive the laser is generated by the Avtech AVN-3-P pulse generator as shown in Fig. 2.7.

The ECL to TTL module amplifies the eight data signals to amplitudes suitable for driving the laser modulators. Its schematic is provided in Appendix C. Fig. 2.13 is a photograph of the complete multiplexer.

2.4 Experimental results

All manufactured pieces of equipment mentioned in this thesis have their brand name and model listed in Appendix A. Throughout the text they are simply referred to as scope, power meter, etc.

Fig. 2.13 Optoelectronic Multiplexer.

Fig. 2.14 shows the experimental set-up used to characterize the output of laser modulator number six. The laser modulator output was characterized with the ANTEL SL1002 PIN detector, the data sheets and frequency response for which, are provided in Appendix B. The PIN responsivity, R, is 0.4 A/W. The equivalent load seen by the photodetector is 50 ohms, which is the input impedance of the scope. The response of the PIN detector to the output of laser modulator number six is shown in Fig. 2.15 in the form of an eye diagram. The peak current calculated from Fig. 2.15 is 80 mV/ 50 ohms.= 1.6 mA. The peak power is the peak current divided by the responsivity or 4 mW. The design requirement for a peak power of 2.7 mW is therefore achieved. The width at the base of the pulse is approximately 1.5 nsec which is also quite close to the design requirement (1.36 nsec).

The time jitter which can be estimated by looking at the thickness of the pulse rising edge is less than 100 psec.

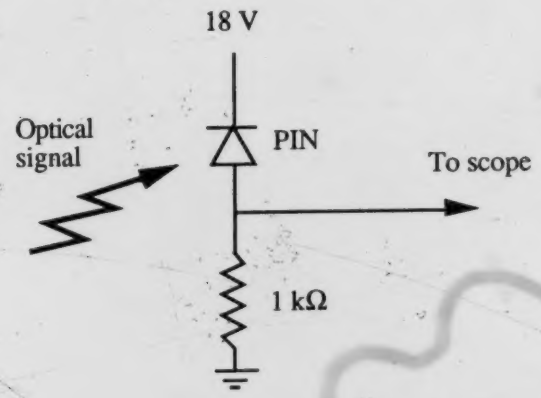

Fig. 2.14 Set-up used to characterize the laser modulator output.

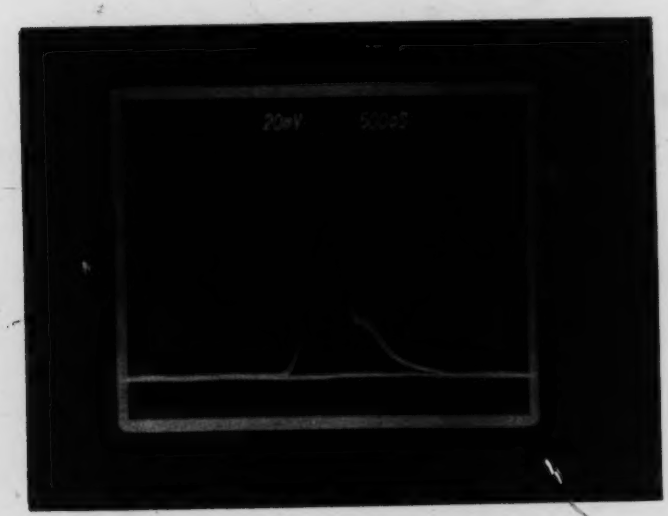

Fig. 2.15 Eye diagram of laser modulator number six.

Fig. 2.16 shows an entire byte of the multiplexed signal which was characterized with the set up of Fig. 2.14 except that the signal was amplified by Amp. # 3 which has a gain of 21 dB. The frequency response of Amp # 3 is shown in Appendix C.

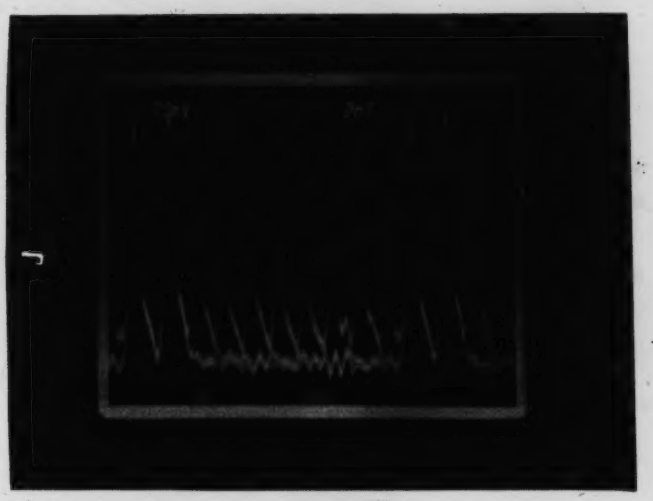

Fig. 2.16 Multiplexed signal.

The taller pulses in the figure are the synchronization pulses and their calculated peak power is approximately 530 μW. The amplitude of the data pulses is in the order of 270 μW. The intersymbol interference penalty (ISI) is defined as

$$-20\log(A_2/A_1), \tag{2.7}$$

where A_2 is the eye opening with ISI and A_1 the eye opening without ISI. A_1 is calculated from Fig. 2.15. The opening in that figure is 72 mV which is reduced by the loss incurred from the star coupler (11.3 dB). Thus, A_1 is 5.3 mV. A_2 is calculated from Fig. 2.16 to be 4.5 mV taking into account the amplification of 21 dB. Equation 2.7 yields 20log(4.5/4.3) or 1.4 dB for the ISI penalty.

These results prove that optoelectronic multiplexing is a viable approach at a bit rate of 560 Mb/s. The performance of the multiplexer could have been improved by using a faster laser. It is possible to produce RZ optical data pulses with widths less than 100 psec by directly modulating a laser diode [14]. The maximum number of channels in a multiplexer is given by

$$1/(BW) \tag{2.8}$$

where B is the baseband channel bit rate, and W the width of the RZ optical data pulse. The maximum number of channels is achieved by making the width of a bit equal to a time slot on the multiplexed bit stream so that there is no guard time between each bit. With B = 1 Gb/s and W = 100 psec for instance, 2.8 yields

$$1 / (1 \text{ Gb/s } 100 \text{ psec}) = 10 \text{ channels.}$$

Two of the channels are allocated for the synchronization pulses and the remaining eight are data channels. The multiplexed bit rate is 8 x 1 Gb/s or 8 Gb/s. Optoelectronic multiplexing thus seems feasible up to almost 10 Gb/s.

The multiplexed bit rate reported for OTDM using fast optical switches by R.S. Tucker is 16 Gb/s [8]. The optoelectronic multiplexer presented in this chapter does not use expensive optical switches and appear to be a more cost efficient approach.

CHAPTER 3

OPTOELECTRONIC DEMULTIPLEXING

This chapter presents a novel optoelectronic DEMUX which is based on two concepts: Switched photodetectors and coincidence gating. In the first part of the chapter the DEMUX is explained conceptually. In the second part the concept of switching photodetectors on and off with a short electrical pulse called the gating pulse is presented. In the third part coincidence gating as a means to extract the gating pulse from two multiplexed data streams is explained and investigated experimentally.

3.1 Optoelectronic DEMUX

The optoelectronic DEMUX, as shown conceptually in Fig. 3.1, is the complement of the MUX. The multiplexed data stream is split 10 ways using a passive star coupler. Passive optical delays are used to synchronize the resulting 10 multiplexed pulse streams. The sum of the time delays at the MUX and the DEMUX for a particular channel is constant and equal to 9 UOD. This ensures that the initial relative timing of all channels is restored at the DEMUX. The relative timing of the pulse streams for all 10 channels is shown in Fig. 3.1. The timing of the pulses is such that the top two photodetectors will only turn on simultaneously when the two synchronization pulses are present, at which point all the data pulses are correctly time aligned at their appropriate channel. At this time, all other photodetectors are switched on and receive their appropriate data pulses. It is noteworthy that a delay of 1.5 UOD between two consecutive bytes ensures that no other pulses except the two synchronization pulses will turn on the top two photodetectors simultaneously.

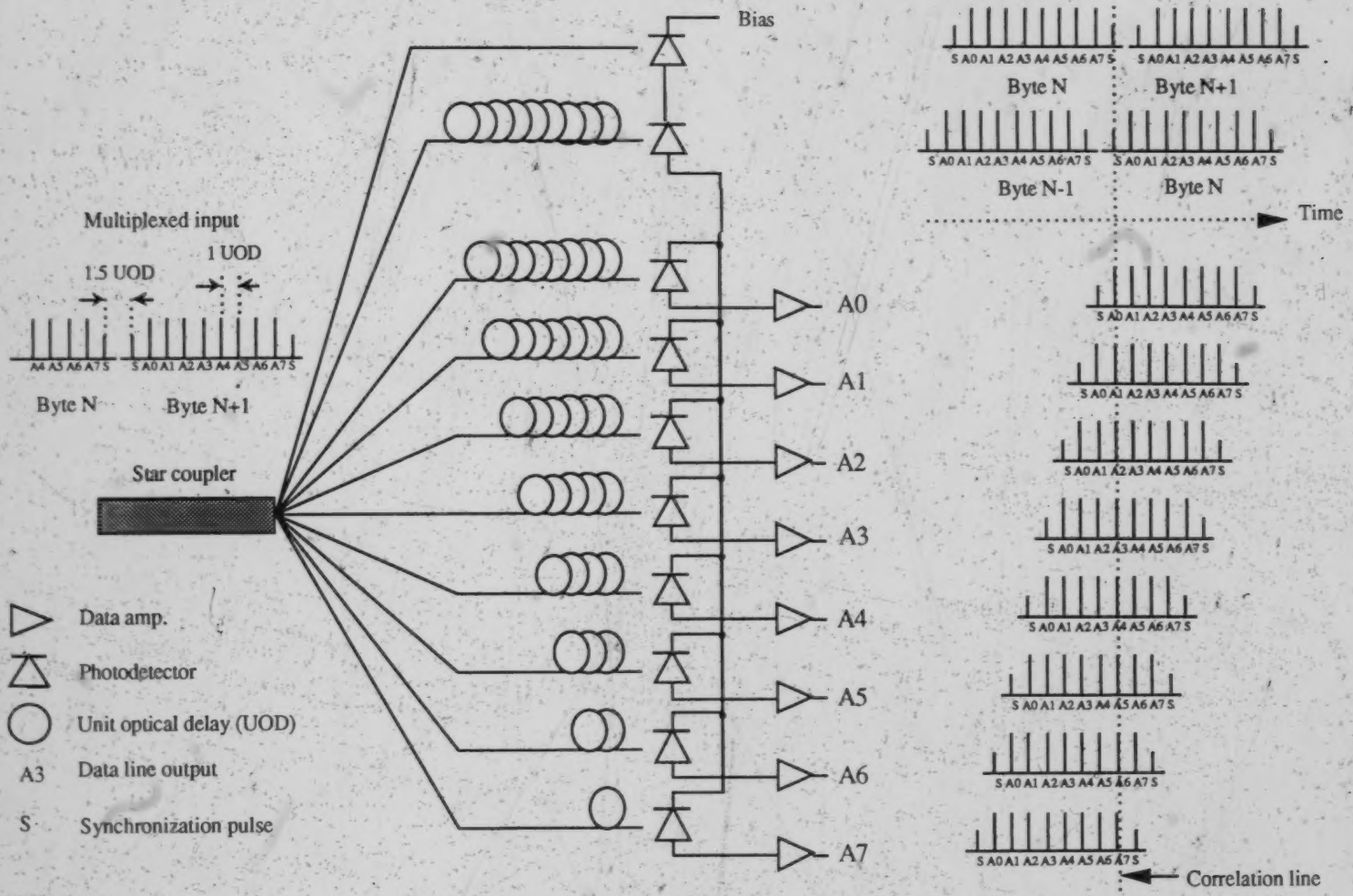

Fig. 3.1 Optoelectronic DEMUX

This optoelectronic DEMUX has three advantages over its optical counterpart. First, no clock recovery circuit is used. Second, it does not use expensive optical switches. Third, it does not require a synchronization circuit.

3.2 Switched junction photodetectors

The idea of switching detectors on and off has been used in optoelectronic switches since it was proposed in 1978 by MacDonald and Hara [14]. Switching is realized by changing the detector bias to render the detector either sensitive or insensitive to light. In the case of a PIN diode, for instance, it consists of changing the bias from reverse to forward, to go from an "ON" state to an "OFF" state.

The most important features of a switched detector are its on/off transition time and its isolation. The isolation is the ratio of the detector's response to a given optical signal when in the on state to that in the off state. The isolation is determined by how much the sensitivity of the detector is reduced by changing its bias. The reduction in sensitivity is dependant on three processes. The most effective, which occurs in all junction photodiodes, is the reduction of the internal impedance of the detector from a very high impedance when the photodiode is reverse biased to a very low value in forward bias. A simplified model for a photodiode is a current source shunted by its internal impedance. As a result, a reduction in internal impedance due to forward bias diverts the photogenerated current from the load thereby reducing the photoresponse. The second process by which sensitivity is affected is the loss of avalanche gain when an APD is under forward bias. The third process is the direct reduction of the quantum efficiency of photodiodes in forward bias, due to the narrowing of the depletion region as a result of heavy injection [15].

The other important feature of a switched photodetector is its on/off transition time, defined as the time it takes for a detector to go from an on state (maximum sensitivity) to an off state (minimum sensitivity). The transition time depends on how fast stored charge can be removed from the depletion layer capacitance of the detector.

3.2.1 Switched photodetection for demultiplexing.

In a time-multiplexed signal each baseband channel is allocated specific time slots. If an optical multiplexed signal is incident on a permanently biased photodetector the electrical output will be simply the detector response to the multiplexed signal. However if the photodetector is biased (turned ON) only during specific time slots that have been allocated to a single baseband channel, the electrical output will be the detector response to that channel. The operation of extracting specific bits from a high-speed multiplexed data stream to reconstruct the original low speed channels is indeed demultiplexing.

A system for demultiplexing an optical signal in the 560 Mb/s range into electronic channels of 70 Mb/s is shown in Fig. 3.2 (a) If a gating pulse hits the array of photoconductors in coincidence with the optical data signal, an electrical version of the data is generated, which, after amplification, flows out the demultiplexed electronic channel. As shown in Fig. 3.2 (b), it is crucial that data and gating pulses be perfectly aligned in time and that the gating pulse full width be less than the data pulse width. Failure to meet these conditions will result in crosstalk, and therefore a higher BER.

3.2.2 Choice of detector

Photodiodes are very effective as moderate-speed optoelectronic switches, but problems are encountered in reducing the switching time below roughly 100 nsec.

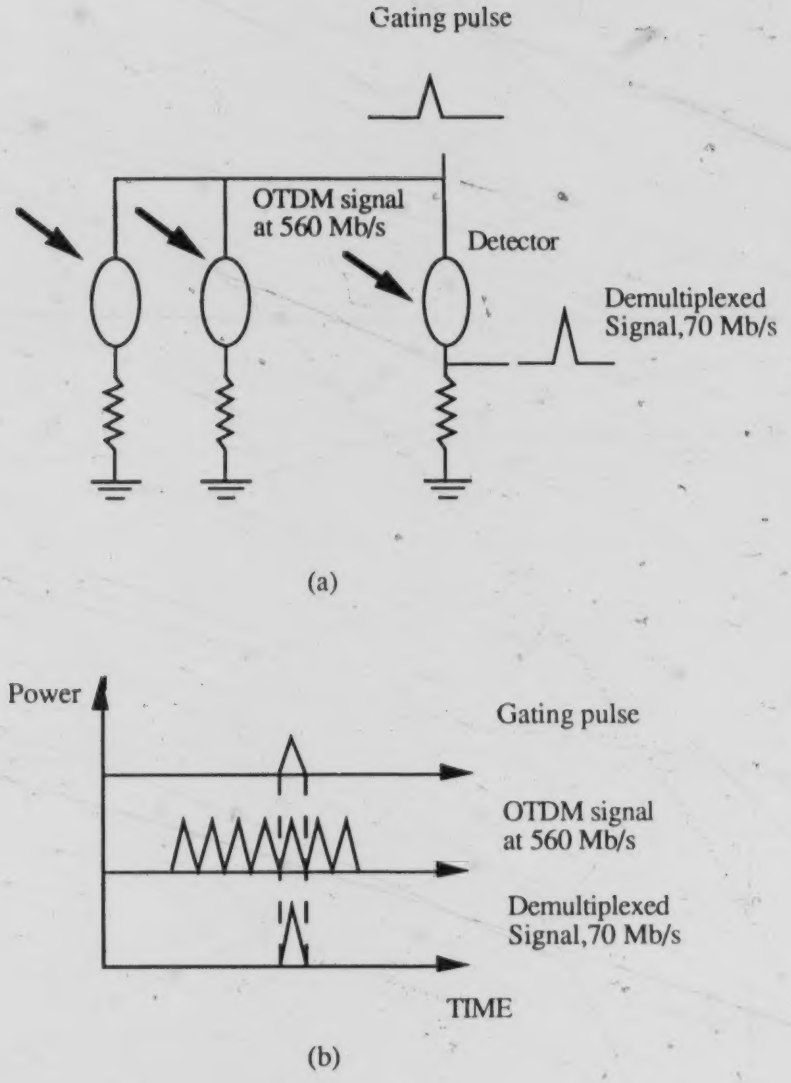

Fig. 3.2 (a) Demultiplexing using switched photodetectors.

(b) Relative timing of the data signals and gating pulses.

The use of a forward bias to establish the "OFF" state is precluded because charge stored in the junction under forward bias cannot be removed sufficiently rapidly through the load when the diode is switched on. Only photodiodes which exhibit a significant reduction in sensitivity at zero bias are usable. The choice is therefore limited to avalanche

photodiodes, or to special photodiodes employing heterojunctions whose internal potential interferes with the quantum efficiency of the device under reverse bias [16]. Both types exhibit switching times of 20 to 30 nsec [17,18]. Because the width of a bit is 1.36 nsec, the required switching time is in the order of a nanosecond. It is therefore impossible to use today's photodiodes in a gigabit OTDM system. Even with improved switching times, photodiodes need gating voltages of the order of 50 to 200 V on a nanosecond time scale and this would be nearly impossible to realize.

Because most p-n junction detectors have very slow switching times due to charge storage, other detectors such as Metal Semiconductor Metal photodiodes (MSMs) and photoconductors appear as better contenders. MSMs are made of only n type material and do not have a p-n junction.

For full sensitivity MSMs require a bias voltage in the order of four to six volts and have an isolation of 50 db at zero volt bias [19]. Such voltage swings are relatively easy to obtain even with subnanosecond rise times. MSMs have reported bandwidths in excess of five GHz [19], which is well above the 700 MHz bandwith required for this experiment. For all the above mentioned reasons, MSMs were used in this experiment.

3.2.3 The MSM photodiode

A cross sectional view of the structure of an MSM is shown in Fig. 3.3.

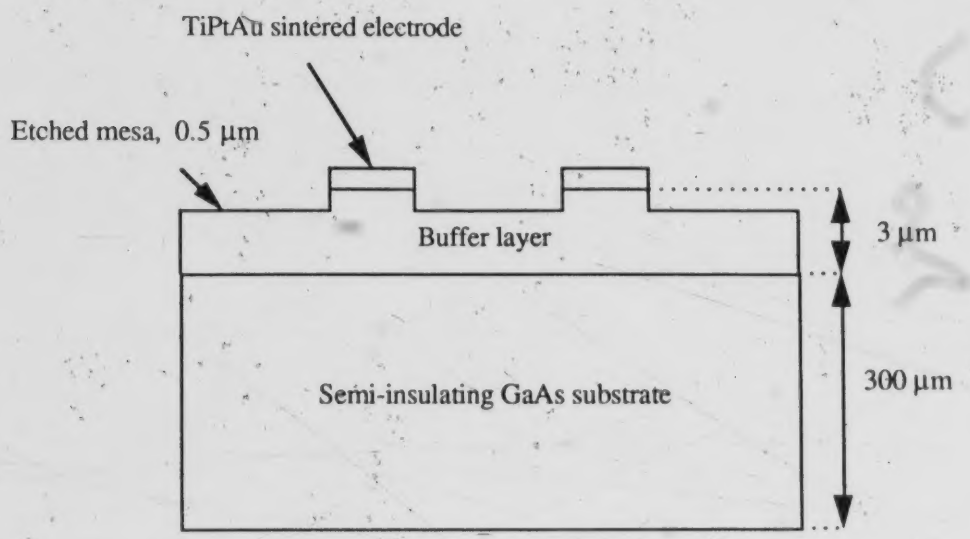

Fig. 3.3 MSM cross sectional view.

The MSM consists of two integral opposed Schottky barrier diodes formed by interdigitated metal (Au, Pt, Ti) cathodes and anodes deposited onto a GaAs epitaxial layer. It is biased so that one Schottky contact (cathode) is reverse biased and the other (anode) is forward biased. The MSM is a completely bidirectional device. Most electrons and holes are generated within the light penetration depth, which is approximately the inverse of the absorption coefficient. For GaAs, the penetration depth is about 1 μm for a wavelength of 0.87 μm [20]. Photogenerated carriers are swept out from the gap by the electric field created by the bias, producing the photocurrent. A responsivity of 0.32 A/W has been reported [19].

3.2.4 Design of MSM

The MSMs were fabricated from a wafer with a 3 μm thick undoped buffer layer with a carrier density of 5E14 /cm^3 grown onto a semi-insulating GaAs substrate (Fig. 3.3). The wafer received a TiPtAu metallization which was sintered to give a Schottky barrier. A 0.5 μm mesa was etched into the buffer layer to form the active area. An

interdigitated structure with an active area of 10^4 μm^2 was chosen for this experiment as shown in Fig. 3.4.(a). The active area dimension insures maximum coupling with the 50 μm core fibre. The anode to cathode distance, which is the spacing between adjacent fingers is 5 μm, and the finger width is 3 μm. The small finger spacing allows for the rapid collection of carriers photogenerated in the GaAs, and hence for high bandwidth. On the other hand the bandwidth is obtained at the expense of quantum efficiency which is reduced by shadowing of the active region by the metal fingers.

Fig. 3.4 (b) shows the array of detectors. The spacing between each of the eight individual detectors is 250 μm.

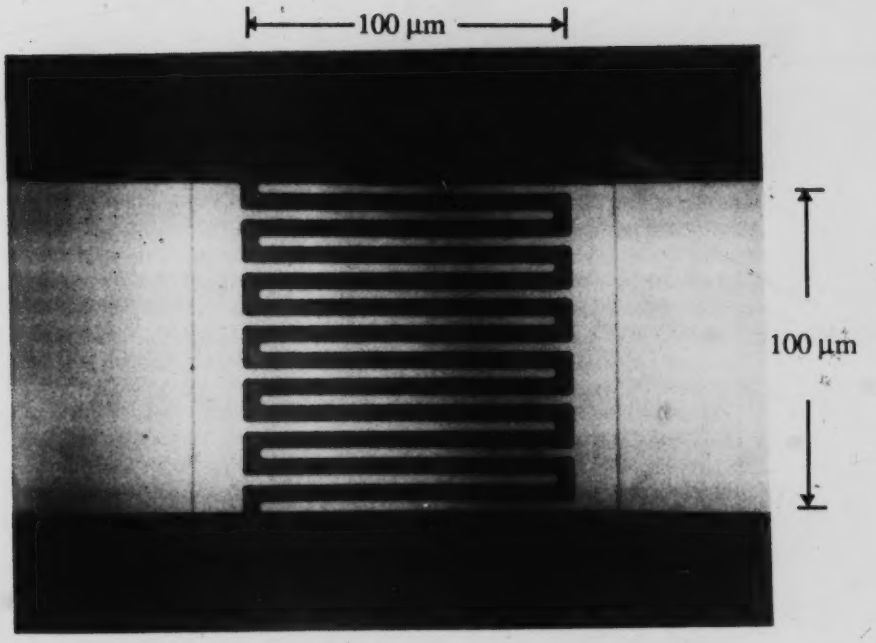

(a)

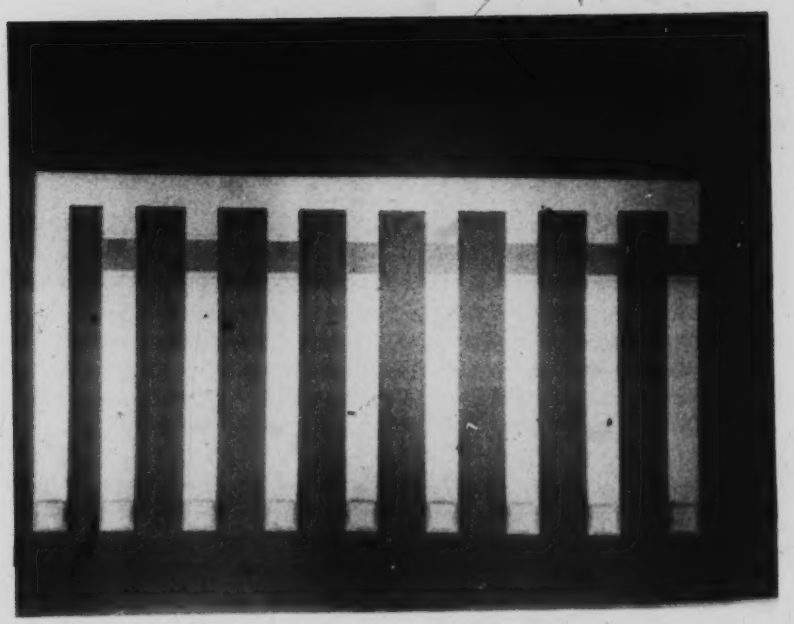

(b)

Fig 3.4 (a) MSM interdigitated structure.

(b) Array of 8 MSMs.

3.2.5 Characterization of MSM

Fig. 3.5 shows the experimental set-up used to determine the frequency response of the MSMs. The laser (ML6411A) was biased at its operating point (I = 62 mA) and its output was measured to be four mW using a power meter. The output of the network analyzer was a sinusoidal current with a peak value of 1.59 mA. The slope of the laser characteristic was measured experimentally to be 0.16 mW/mA.

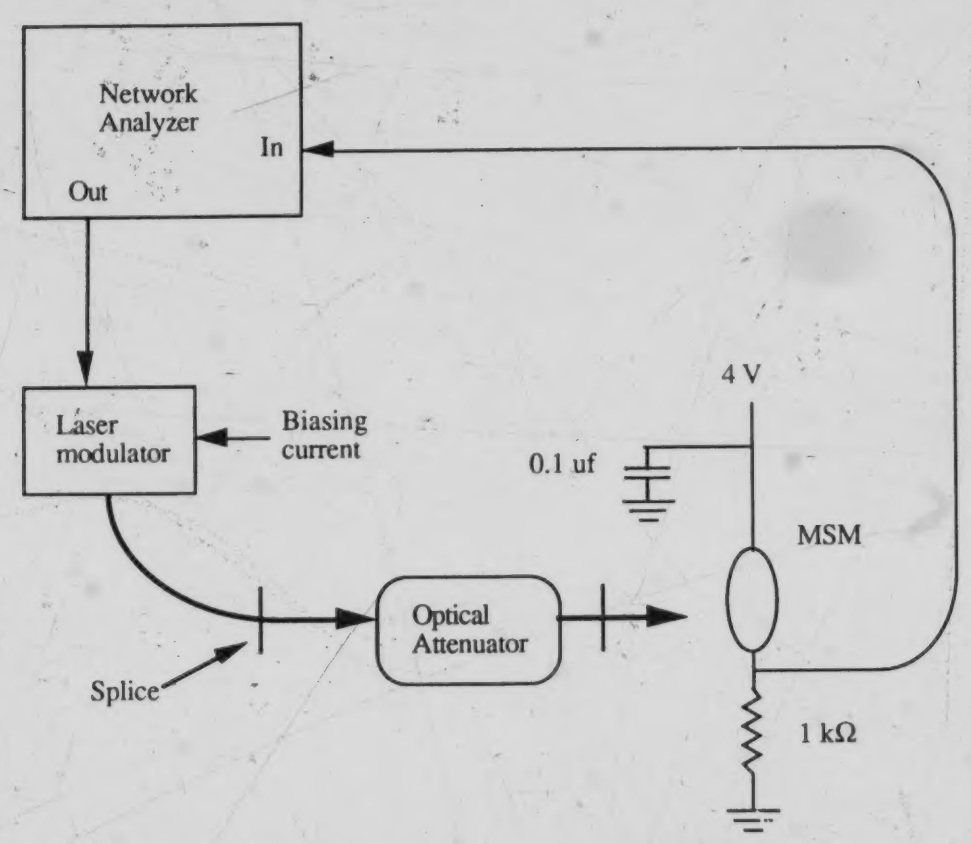

Fig. 3.5 MSM frequency response measurement

Therefore the peak excursion of the laser output power was 1.59 mA x 0.16 mW = 0.254 mW. The modulation depth, which is defined as the ratio of the maximum excursion and the average power , was found to be

0.254 mW / 4mW = 0.0635 or 6.35 %.

The anticipated peak power at the detector was 350 μW. Therefore this power level was used to characterize the detectors. There was no coupling loss between the fibre and the detector because the detector interdigitated area was much bigger than the radiation pattern of the light from the fibre. The flattest frequency response curve was obtained with a bias of four volts or greater. The effective load seen by the MSM is the input impedance of the network analyzer (50 ohms). Fig. 3.6 shows the measured frequency response. With a 3 dB cut-off frequency of about three GHz as shown in Appendix A the laser had very little influence on the overall frequency response. It can be concluded that Fig. 3.6 represents the frequency response of the MSM. The usable frequency range of the detector is estimated at 2 GHz beyond which there is a sharp drop in the response.

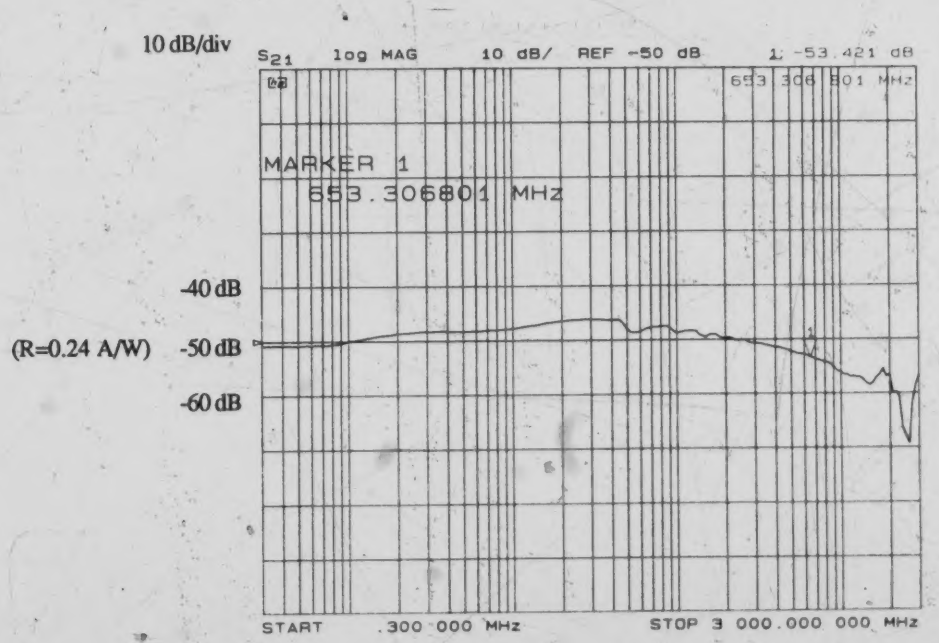

Fig. 3.6 MSM frequency response

The experiment was repeated to obtain the response of three more detectors out of the same array. The results were very similar. Another very important characteristic of a detector is its responsivity. Two responsivity measurements were made, one at DC and the other at 560 Mb/s, both with a four volts bias on the detector. The DC measurement was made as follow. A power level of one mW was measured at the output of the fibre using the power meter. This power incident on the MSM produced an output of 12 mV into a 50 ohm load. The DC responsivity is therefore

(12 mV / 50 ohm) / 1 mW = 0.24 A/W

For the second measurement, an optical pulse with a full width of 1.4 nsec and a peak power of 1.26 mW was incident on the MSM. The power was measured with the SL1002 PIN detector with responsivity 0.4 A/W. The equivalent load seen by the MSM was 25 ohms. Amplifier # 3, which has a gain of 21 dB, was used to amplify the output. The peak amplitude of the resulting pulse was 64 mV giving a detector output current of 64 mV / 25 ohms / 11.2 = 0.114 mA. The high frequency responsivity is therefore

0.114 mA / 1.26 mW = 0.09 A/W,

which is in rough agreement with Fig. 3.6.

3.3 Coincidence gating

Coincidence gating is the extraction of the coinciding parts of two signals or patterns using an AND gate. The relative timing of the two input signals is important because it determines precisely what is going to be extracted. The proper timing is achieved by introducing a delay in one the input signal paths. When working with optical signals such delays can be implemented using optical fibre as described in Chapter 2.

The concept proposed here is to use a coincidence gate to extract the gating pulse from the multiplexed signal. Fig. 3.1 shows the proposed scheme in the context of an eight channel system. Gating pulse extraction is achieved by having two permanently biased photodetectors in series (AND gate) which await the two synchronization pulses. Optoelectronic AND gates made using two photodetectors in series have been reported with subnanosecond resolution [20].

3.3.1 Choice of detector

The bandwidth required for the AND gate depends on the frequency content of the synchronization pulse. The pulse has a full width half maximum of 600 psec. The bandwidth required as observed on the spectrum analyzer is approximately 1.4 GHz. The SL1002 PIN detector was chosen for its high responsivity (0.4 A/W) and wide bandwidth (1.7 GHz) to perform the AND gating function. Two of them were mounted in series as described in the next section.

3.3.2 Description of the coincidence gating experiment

The two PIN diodes were mounted in a high frequency package. Both electrical connections PIN/package were made with conductive epoxy while the PINs were wire bonded together, as shown in Fig. 3.7. The package was put in a high frequency test jig for performing the experiment. Fig. 3.8 shows two micro-manipulators holding the output fibres above the test jig. A microscope was used to position the fibres exactly onto the detectors.

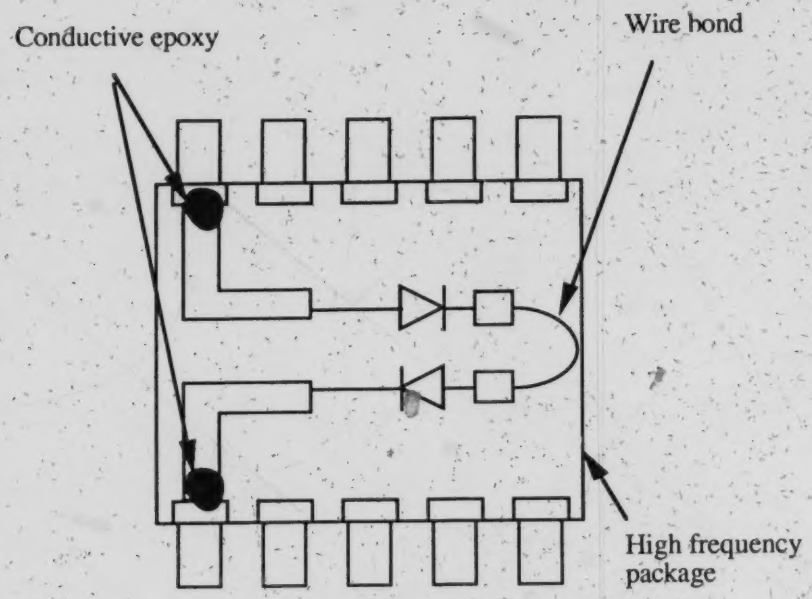

Fig. 3.7 Optoelectronic AND gate

Fig. 3.9 shows the experimental set-up. Fibres F1 and F2 are the top two fibres in Fig. 3.1 and their outputs are shown in Fig. 3.10 and 3.11. Fig. 3.12 shows the relative timing of the pulses coming out of fibre F1 and F2 and the expected electrical output of the AND gate. A delay of nine UODs was introduced on F2 so that the synchronization pulses from both fibres correlate to produce the gating pulse. As can be seen in Fig. 3.10 and 3.11 no data were multiplexed with the synchronization pulses as the first attempt to prove the concept of correlation detectors. The peak power of the pulses is about 750 μW, their width 1.4 nsec, and the repetition rate is 70 MHz.

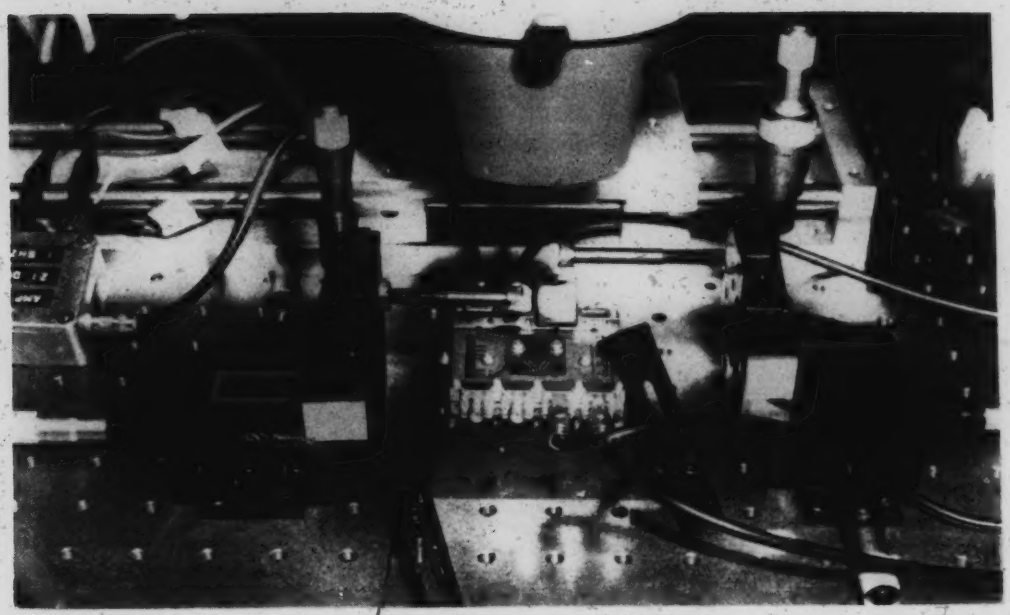

Fig. 3.8 Test jig and micro-manipulators

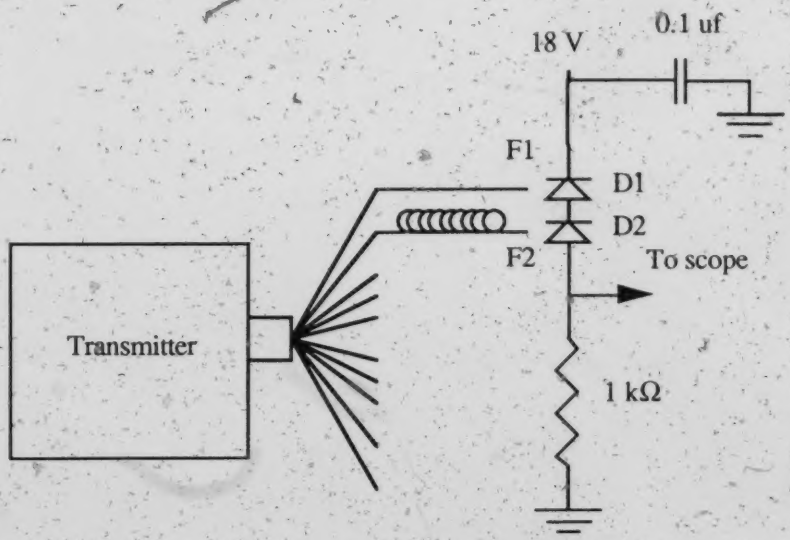

Fig. 3.9 AND gate experiment

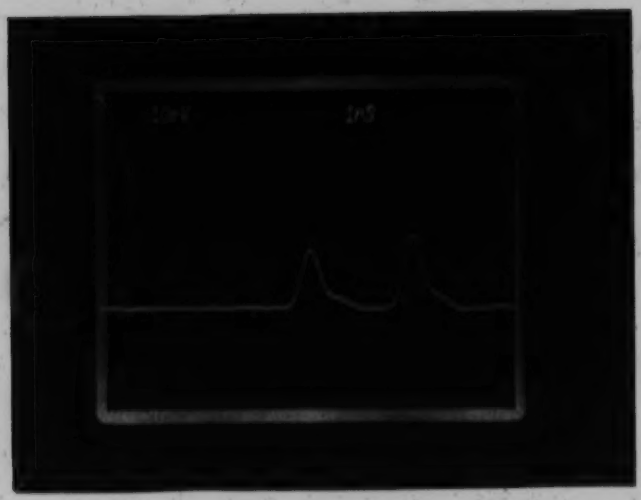

Fig. 3.10 Output from fibre F1

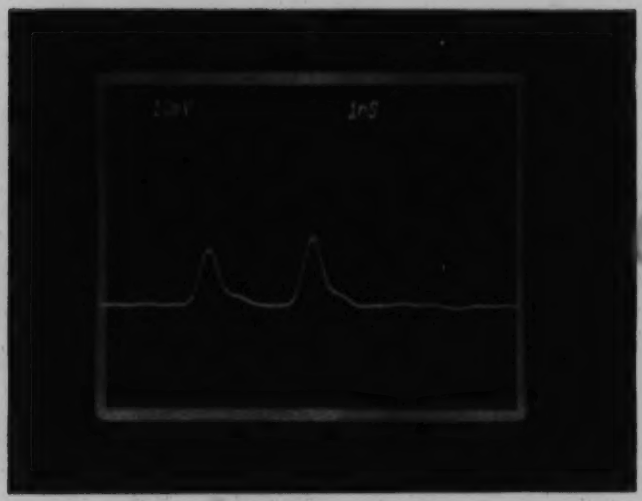

Fig. 3.11 Output from fibre F2

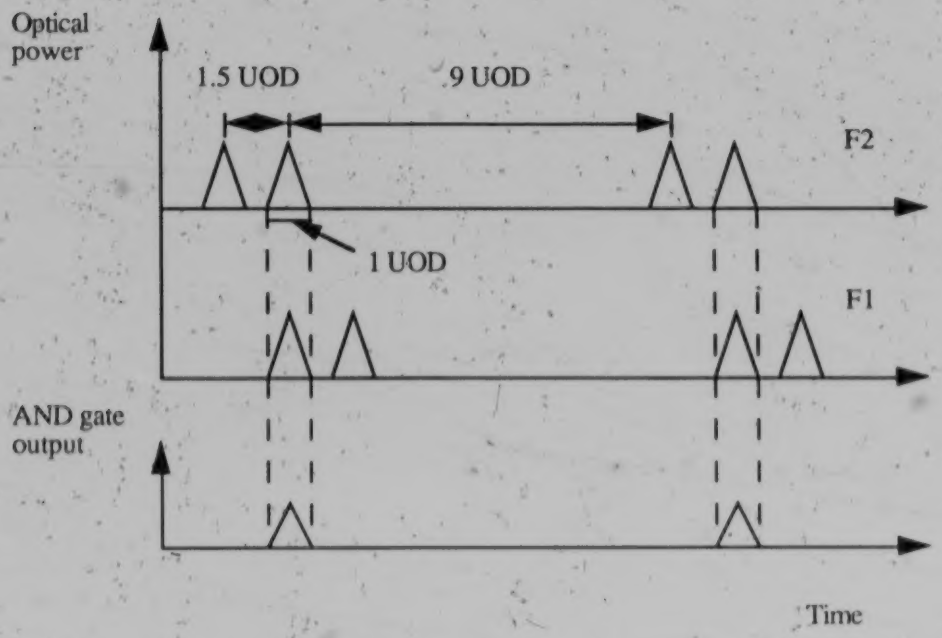

Fig. 3.12 Inputs and EXPECTED output of the optoelectronic AND gate.

3.3.3 Discussion of results

Fig. 3.13 shows the output of the optoelectronic AND gate. This picture suggests that the recovery time of the PIN diode is too slow. The recovery time is defined as the time it takes to go from forward to reversed bias [21]. In fact, detector D2 remains permanently forward biased acting as a short circuit and letting the signal on detector D1 dictate the shape of the output. The experiment was performed again with an elapsed time between two adjacent pulses (t1) increased to 10 nsec. This did not produce any noticeable at the output. It can be concluded that the recovery time of the SL1002 PIN is greater than 10 nsec.

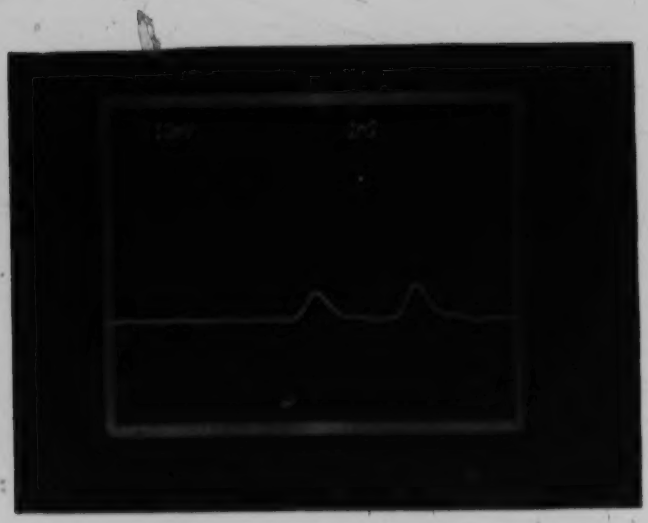

Fig. 3.13 Optoelectronic AND gate output

3.4 Threshold detection as an alternative method for coincidence gating

Let us assume a perfectly working optoelectronic AND gate and repeat the coincidence gating experiment with data and synchronization pulses. Fig. 3.14 shows the optical inputs and the expected electrical output. As one can see, data and synchronization pulses from the two inputs partially coincide. The result is a corrupted gating pulse that requires threshold detection before it can be used to activate switched photodetectors. Degeneration due to data overlap can be avoided if the width of the data and the synchronization pulses is halved therefore doubling the bandwidth of the signal. Practically the requirements on the pulsewidth are even more stringent since the AND gate has a resolution time that has to be taken into account.

If bandwidth is a limiting factor due to the laser or the electronics it is more attractive to send only one synchronization pulse per frame and to use threshold detection to

extract the gating pulse. Threshold detection at high frequency can be performed using GaAs MESFETs to clip the undesirable part of the gating pulse stream and even to provide gain that will be required to amplify the gating pulse to a level suitable for switching the photodetectors. Sending only one synchronization pulse has the following advantages: First, as mentioned in the previous paragraph the data pulsewidth can be made larger. Second, removing one synchronization pulse makes it possible to add another data channel without increasing the bandwidth of the signal. Third, the need for a 1 x 2 power splitter at the transmitter no longer exists. For obvious reasons, if the amplitude of the synchronization pulses cannot be made larger than the data then correlation detection becomes the preferred alternative.

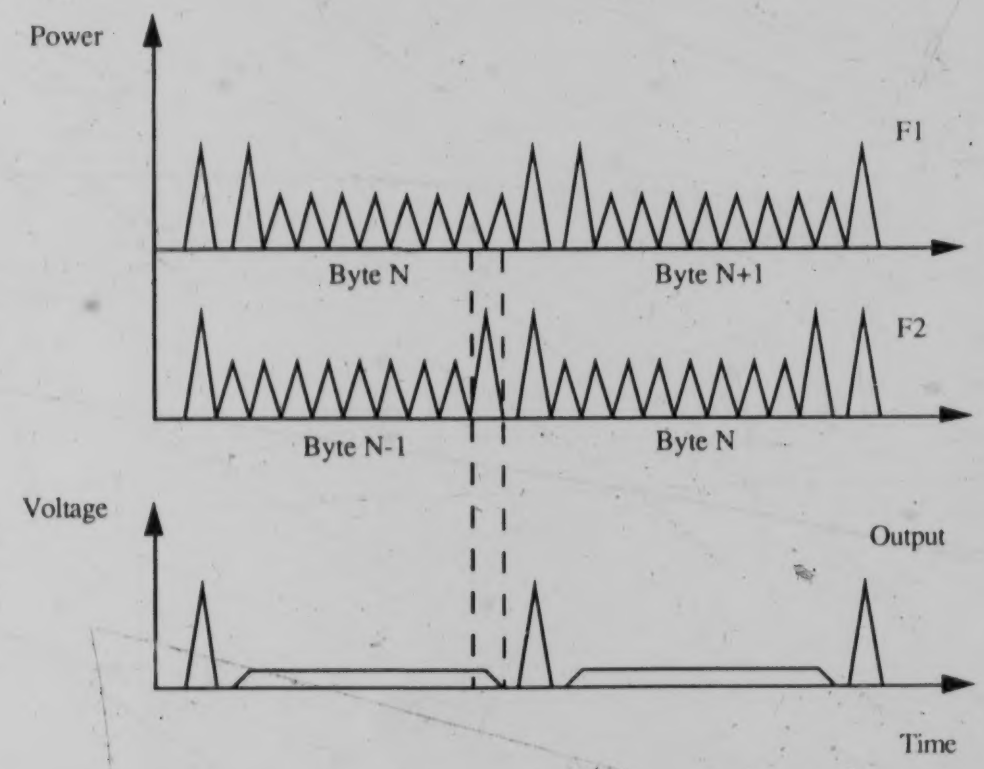

Fig 3.14 Data interference on the gating pulse signal.

CHAPTER 4

DEMULTIPLEXING EXPERIMENT

The purpose of this chapter is to present experimental verification that switched photodetectors are a viable approach for optically time-division-demultiplexing the equivalent of a 560 Mb/s data stream. Two optical data streams are multiplexed on one optical fibre using passive optical delay lines and a 2 x 2 star coupler and are then demultiplexed with MSM photodiodes that are switched on for approximately 1 nsec. BER measurements are taken and the responsivity of the MSM device is measured.

4.1 Multiplexing of two data streams

Fig. 4.1 is a block diagram for the transmission experiment. The output of the data generator is fed into a series of shift registers which create a delay difference between the two laser modulators of 28 bits. The delay was inserted to minimize correlation between the two data streams. The circuitry for laser modulator 1 and 2 is identical to that described in Chapter 2. The data format is RZ, where, the width of a "one" is approximately 1.4 nsec. The data rate is 70 Mb/s and the peak power is 4 mW. The pigtail of laser modulator 1 is fusion spliced to the 2 x 2 star coupler while a delay of 1.36 nsec (1 UOD) is added between laser modulator 2 and input #2 of the power splitter. An identical delay is also spliced at output 3 of the power splitter. The purpose of the power splitter and the delay lines is to multiplex the output of laser modulator 1 and 2. The multiplexing technique is identical to the one used for the transmitter of Chapter 2 - the reader is referred there for the calculation of the UOD and for background information.

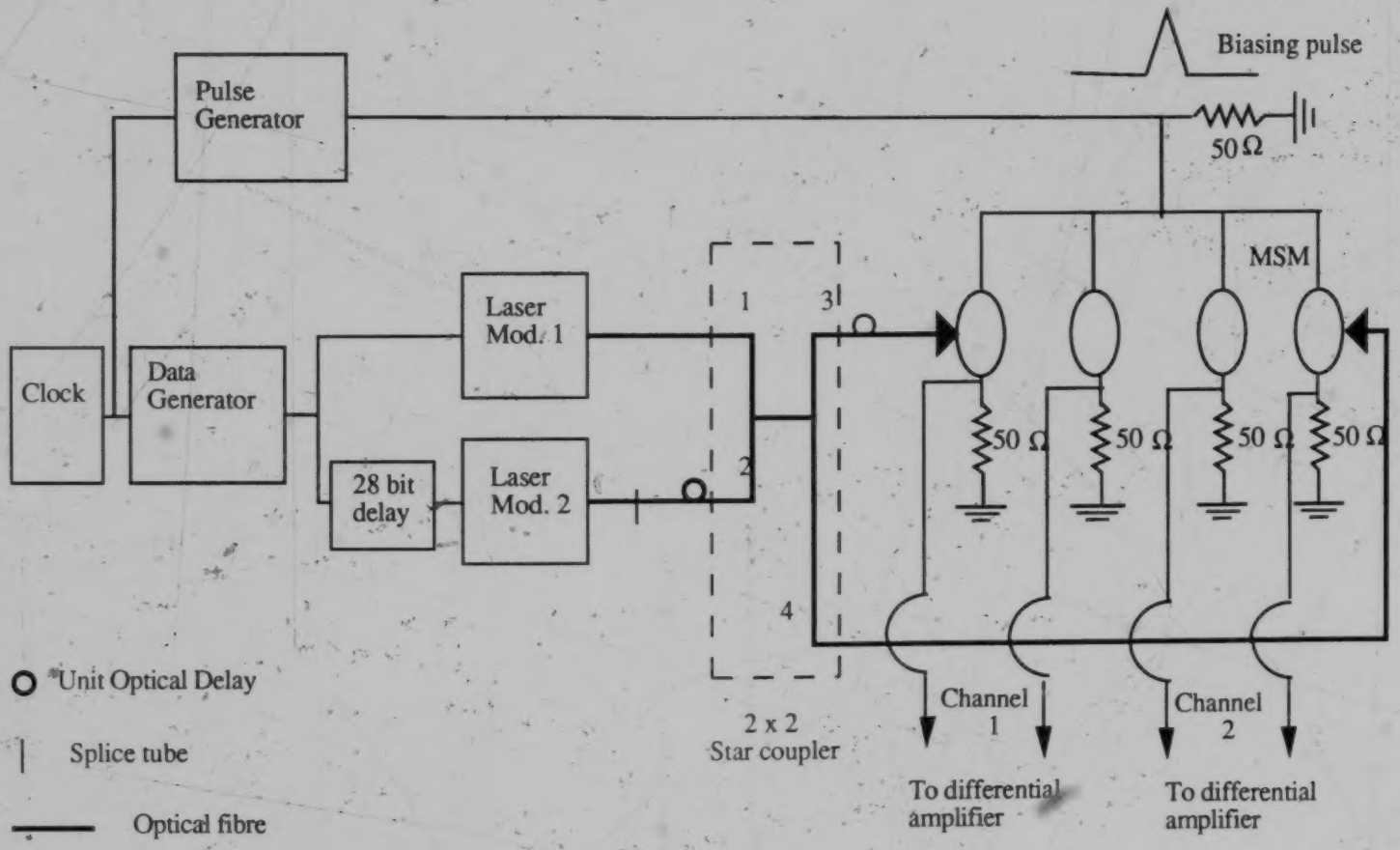

Fig. 4.1 Transmission experiment

Figs. 4.2.1 and 4.2.2 show the eye diagrams of the data coming from output fibre 3 and 4 while fig. 4.3 shows their relative timing. The triangular shaped pulses - all binary "1" for purpose of clarity - are marked 1 and 2 for laser modulator 1 and 2.

Fig. 4.2.1 Output from fibre 3

Fig. 4.2.2 Output from fibre 4

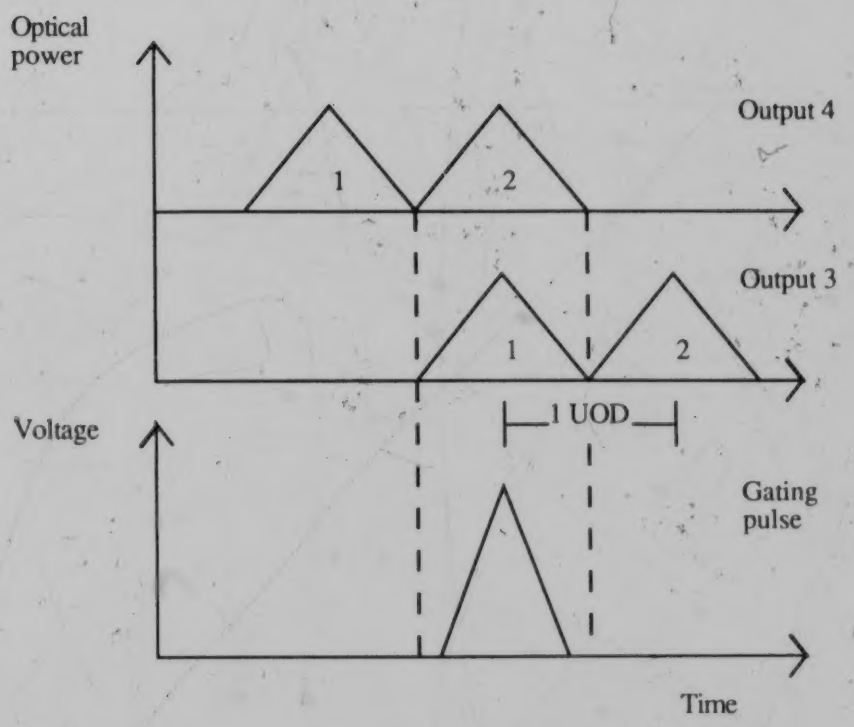

Fig 4.3 Relative timing of data signals and gating pulse.

4.2 Demultiplexing

Demultiplexing with switched photodetectors as explained in section 3.2.1 is achieved by turning a detector on during the appropriate time slot. The four MSMs shown in Fig. 4.1 are part of an array of eight detectors mounted in a high frequency package. For the experiment the package was placed in a high frequency test jig. It is noteworthy that the data and pulse generator share a common clock which ensures perfect synchronization of the data and the gating pulse. The amplitude of the gating pulse is five volts and its full width is one nsec. A 50 ohm resistor is connected between the common point of the detector array and ground to properly terminate the output of the pulse generator.

One of the problems encountered with a switched photodetector is the leakage pulse. This effect is intrinsic to the capacitive nature of the detector. The leakage pulse can be quite large and its effect is shown in Fig. 4.4 where a "zero" is nothing else but the gating pulse leaking through the detector. One efficient way to eliminate that problem is to utilize an MSM with no light incident on it, as shown in Fig. 4.1, to generate a data-independant leakage pulse that is subsequently subtracted from the data using a differential amplifier.

Fig. 4.4 Effect of the leakage pulse on the data

The amplification stages following the photodetectors are shown in Fig. 4.5. A third order Butterworth 70 MHz low pass filter has been added after the differential amplifier to widen the data pulses to seven nsec which is suitable for sampling by the Bit Error Test Set.

Fig. 4.5 Data amplifier stages

The schematics and frequency response for the differential amplifier and the low pass filter are shown in Appendix C. The frequency response of Amp. 1 is also shown in Appendix C.

4.3 Noise calculation

In order to estimate theoritically the BER it is essential to know the total noise power at the receiver output. Four major sources of noise can be identified for the system shown in Fig. 3.1. They are the laser, MSM, load, and differential amplifier. The total noise power was calculated to be 1.66E-8 V^2 and is dominated by the differential amplifier noise which was measured using the spectrum analyzer.

4.4 Experimental results

BER measurements were taken to assess the influence of different factors on the performance of a demultiplexer built with switched photodetectors. The factors considered were the average received power per detector, the addition of one channel, and the amplitude of the gating pulse. In addition the responsivity under pulsed bias was measured. Pictures 4.6.1 and 4.6.2 show the transmitted and received data as well as the eye diagram. The average power received per detector is 107 μW and the BER is 1 E-8.

Sent NRZ data
at system input

Received RZ data
delayed by 38 bits

Fig. 4.6.1 Demultiplexing by switched photodetection

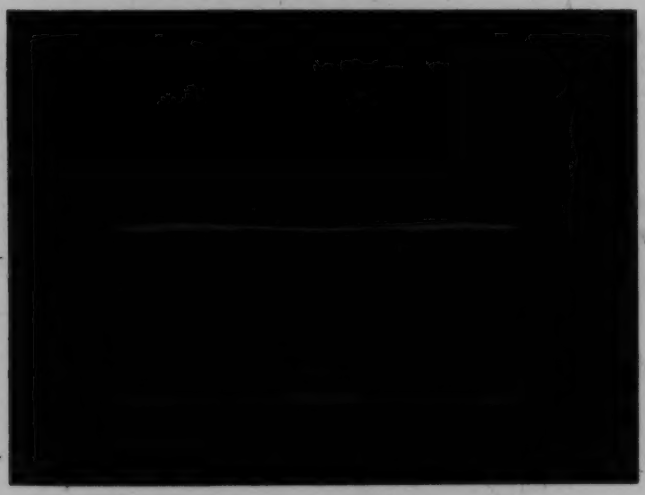

Fig. 4.6.2 Eye diagram of demultiplexed data

4.4.1 Responsivity under pulsed bias

The responsivity was calculated from Fig. 4.6.2. The average voltage over a bit period (13.6 nsec) was estimated graphically to be = 0.81 V. The total gain of the demultiplexer was 63.4 dB or 1479 so the average output current of the MSM was

0.81 V / (1479 x 25 ohms) A = 21.9 μA,

where 25 ohms is the equivalent load seen by the MSM.

The average optical power of the data pulse is 133 μW. This figure was obtained by measuring the peak power of the data pulse with a similar set-up to Fig. 2.14 except that an MSM was used instead of a PIN. The average power was then calculated using eq. 2.6. The MSM responsivity under pulsed bias was

21.9 μA / 133 μW = 0.16 A/W.

This figure is higher than what was measured for a four volt DC bias with an optical pulse of the same shape (see section 3.2.5). The responsivity in that case was calculated to be 0.09 A/W. It appears that a pulsed bias enhances the responsivity of an MSM and an explanation for this has not been found yet. This higher value of responsivity will influence the BER for a given power. For a BER of 10^{-6} the required signal voltage to noise voltage ratio is 92.2[22]. Because the noise voltage was 1.29E-4 V (see section 4.3) the peak to peak signal must be

1.29E-4 V x 92.2 / 25 ohms = 0.48 mA.

The peak power required is 0.48 mA / 0.16 A/W = 3 mW. Using eq. 2.6 the average power required is 3 mW / 21 = 143 μW.

4.4.2 BER measurements

A pseudo-random pulse generator producing a sequence of length 2^9 was utilized to perform all BER measurements. The optical power was measured using an MSM with a

DC bias of four volts. Micro-manipulators were used to move the fibre over the active area of the detectors. The BER was slightly unstable so an average had to be taken. The curve labelled "1 channel" on Fig. 4.7 was taken with only Laser modulator 1 activated. The curve labelled "2 channels" was taken from channel 1 with both laser modulators transmitting therefore adding an interfering channel in the next time slot. One can see very little difference between the two curves except at a power of -12.8 dBm. This point for the "1 channel" curve seems to be away from the natural course of the curve and is probably due to the unreliability of the BER measurement. From this supposition we are led to conclude that the two curves are not much different. and that the slight difference is likely due to ISI. This result implies that the detector was indeed turned off by the time the data from the next time slot reached it. Consequently the electrical switching time of an MSM is less than 1.4 nsec (length of a time slot or 1 UOD).

It can also be seen from Fig. 4.7 that a BER of 10^{-6} is achieved with an average received power of approximately -9.5.dBm or 112 μW. This is in rough agreement with the calculation of section 4.4.1 (143 μW) based on the noise power at the receiver.

Fig. 4.8 shows results when data was received at channel 2 with both laser modulators transmitting. This is the situation where an interfering channel is added in the time slot just before the received data. Again the two curves are very similar. A conclusion that can be drawn from Fig. 4.7 and 4.8 is that interfering channels before or after the received data do not significantly affect the BER . Therefore it has been demonstrated that it is possible to use switched photodetection as a demultiplexing technique in a multi-channel system.

Another graph of significance is the BER as a function of the gating pulse amplitude for channel 1 with both laser modulators transmitting (Fig. 4.9). The experimental set-up is again the same (see Fig. 4.1). The average optical power received per detector was

kept constant throughout the experiment at 110 μW. The amplitude of the gating pulse was varied from 1.5 to 5.4 V with a constant width of one nsec. 5.4 V was the upper limit achievable for our pulse generator while keeping the ringing to less than 10 %. The effect of excessive ringing was to turn the detector on again in the following time slot therefore causing significant crosstalk. Fig. 4.9 shows that no error floor was reached. The improvement in performance suggests that the responsivity is proportional to the gating pulse amplitude. This is not surprising since detector responsivity is in general proportional to the level of the DC bias. One very interesting aspect of the curve is that there is no error floor, which suggests that a further improvement in BER is possible simply by increasing the amplitude of the gating pulse.

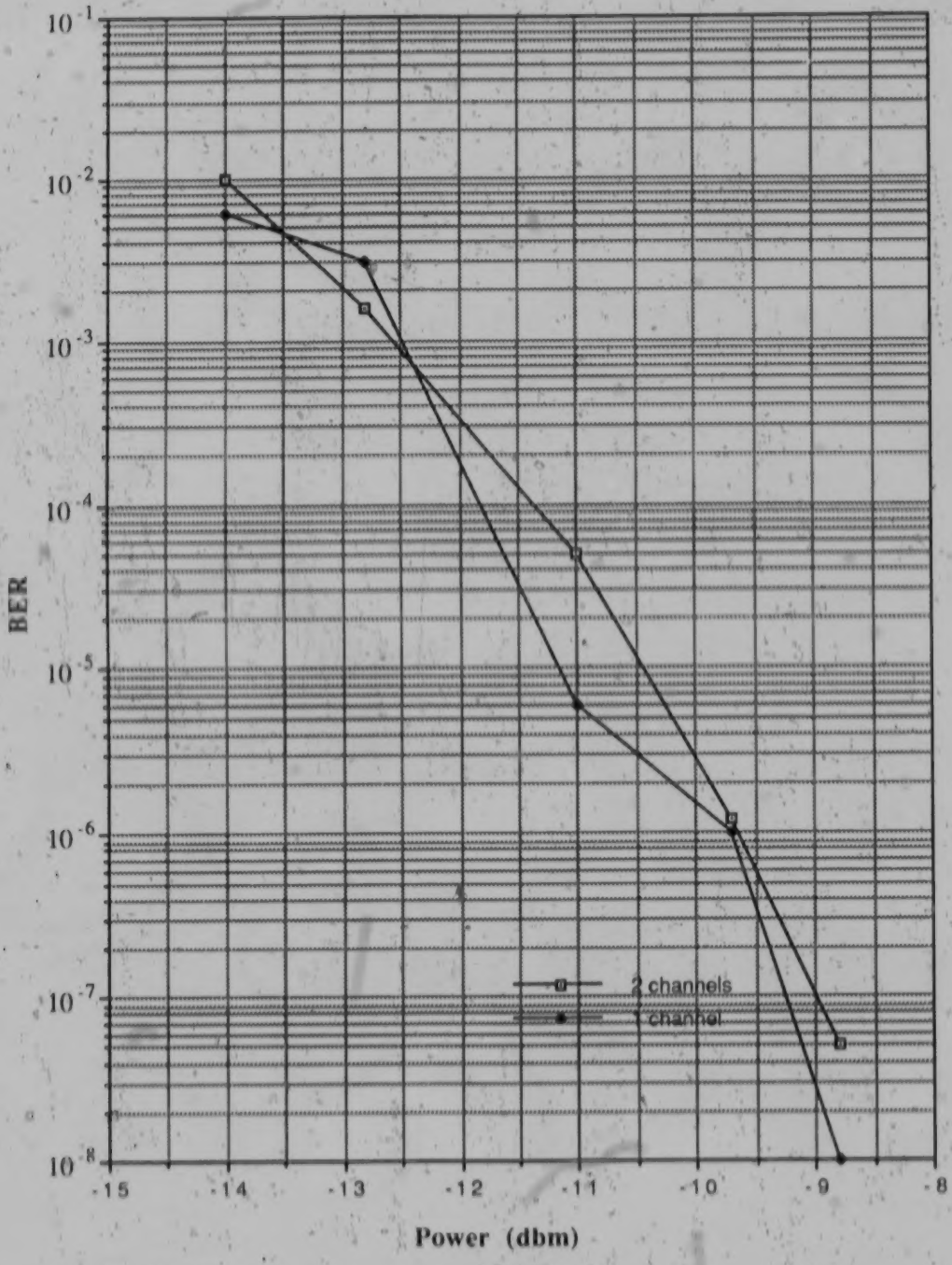

Fig. 4.7 Effect of one additional channel on the BER for Channel 1

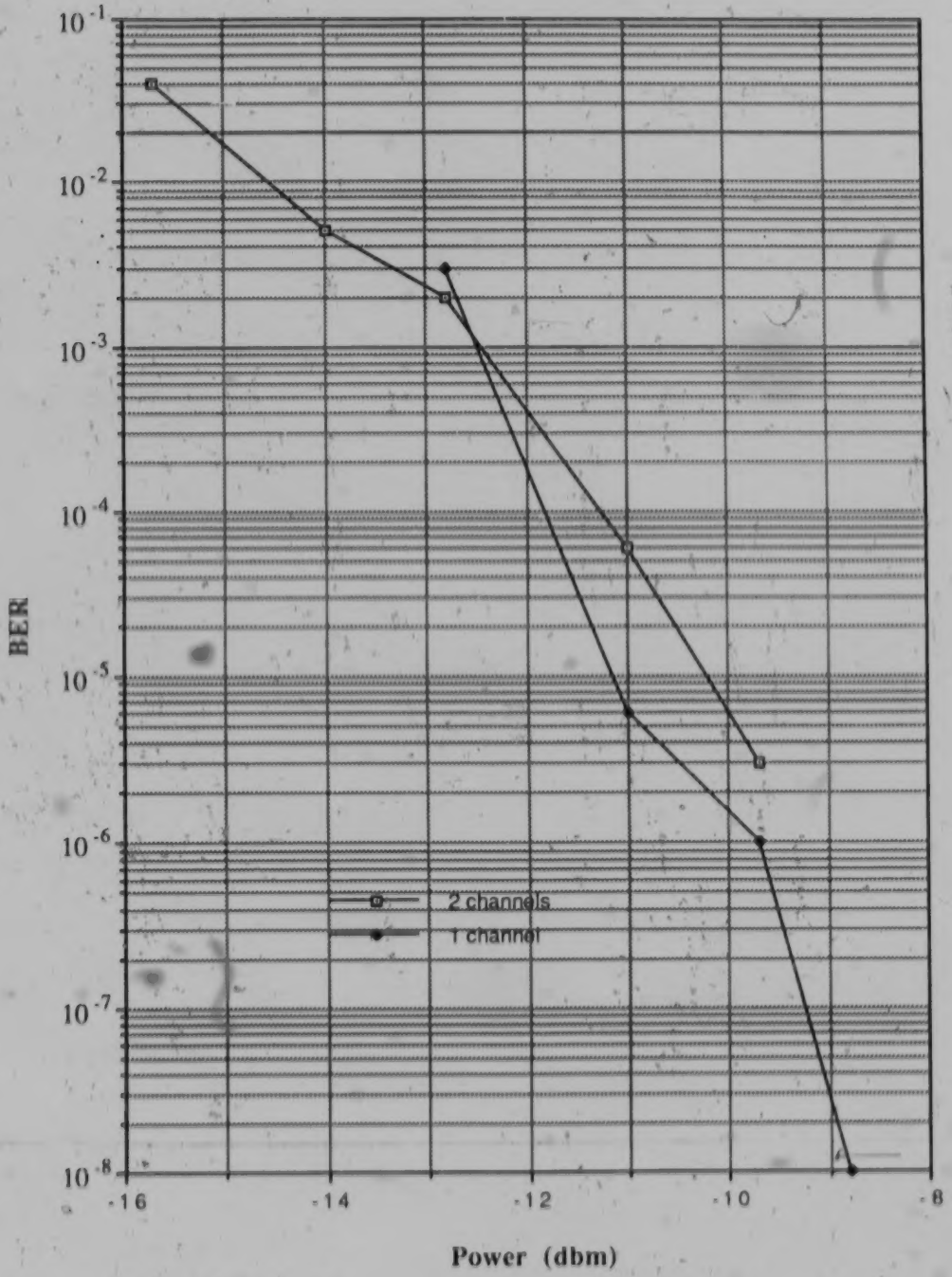

Fig. 4.8 Effect of one additional channel on the BER for Chanpel 2

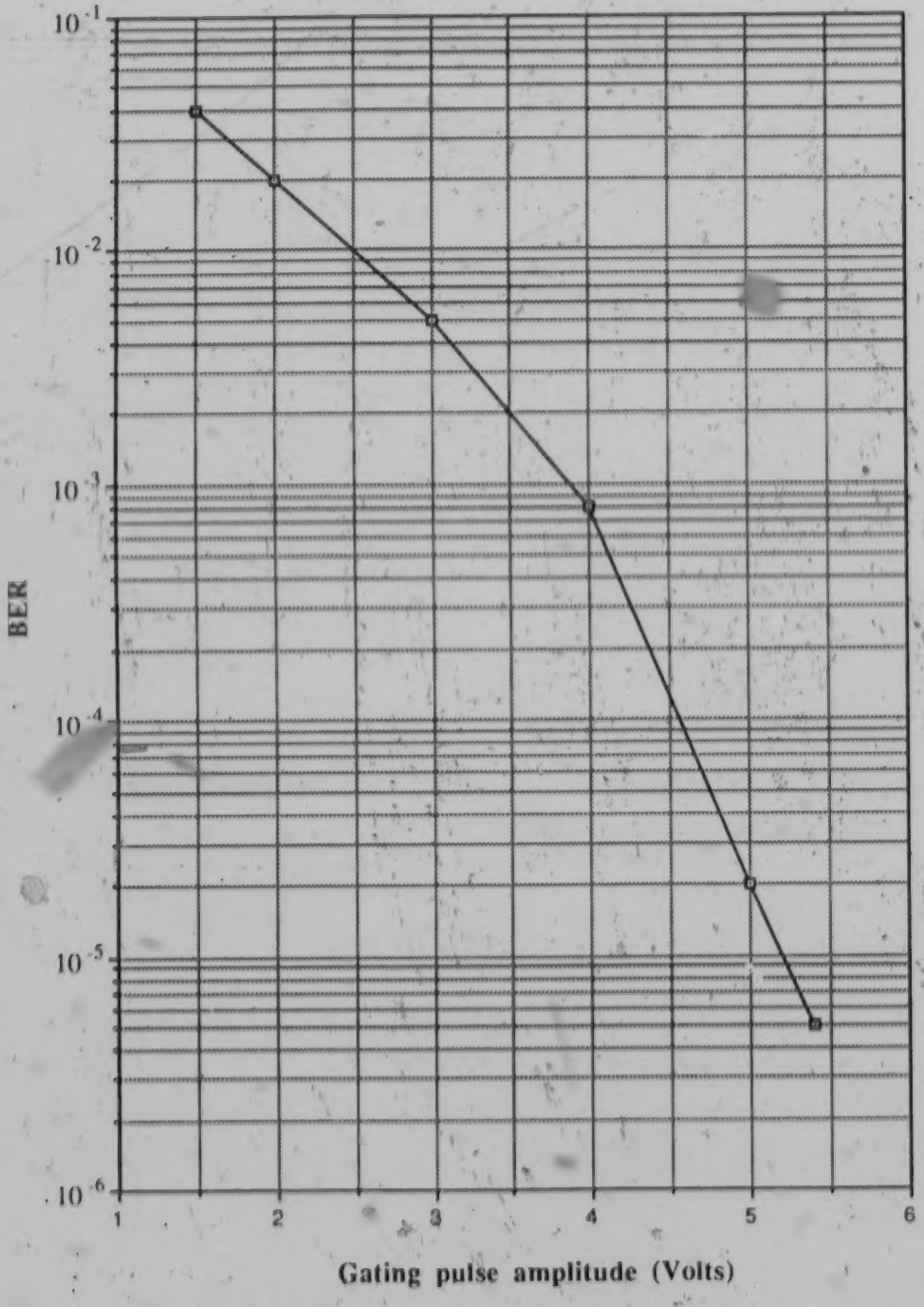

Fig. 4.9 Channel 1 with two active channels

CHAPTER 5

SUMMARY AND CONCLUSION

Novel optoelectronic techniques for time-division multiplexing and demultiplexing have been discussed. These optoelectronic techniques try to capitalize on well developed electronic techniques, and on promising avenues offered by optical devices such as increased bandwidth.

An optoelectronic MUX was constructed and eight channels were multiplexed to produce a multiplexed bit rate of 560 Mb/s using inexpensive lasers similar to the type found in compact disk players. Sampling of the NRZ-baseband electrical data was realized using the threshold characteristic of the laser. The timing and combining of the eight input baseband channels was realized using fibre delays and a passive power combiner. The optoelectronic approach is very simple and more cost efficient compared to optical multiplexing (section 2.4). However the achievable multiplexed bit rate using optoelectronic techniques is limited by the width of the RZ optical data. Using presently available electronics, optoelectronic multiplexers could achieve a multiplexed bit rate of eight Gb/s (section 2.4) whereas the maximum reported bit rate for optical multiplexing is 16 Gb/s [8].

An optoelectronic approach for demultiplexing high bit rate signals was presented. The optoelectronic DEMUX does not use a clock signal to demultiplex the high bit rate data stream. The novel optoelectronic DEMUX is based on two techniques: coincidence gating and switched photodetection.

It was found that coincidence gating may not be the ideal solution for extracting the gating pulse. Coincidence gating requires that the width of the RZ optical data be reduced by at least a factor of two therefore increasing significantly the bandwidth requirements for

the laser modulator. It is preferable to use threshold detection, performed with GaAs MESFETs, to extract the gating pulse from the multiplexed bit stream.

MSMs were switched on for approximately one nsec to demultiplex the equivalent of a 560 Mb/s data stream and a BER of 10^{-8} was achieved. The BER was greatly dependant on the amplitude of the gating pulse. Gating pulses with amplitudes of up to 5.5 V were used and no error floor was observed. The performance of the optoelectronic demultiplexer could be improved by using a low noise amplifier at the receiver and by using MSMs with higher responsivity. Also it should be possible to integrate the MSMs with the front end amplifier.[1]. Integrated receivers with fewer parasitic elements should allow demultiplexing at higher multiplexed bit rates.

Based on the experimental results obtained, the optoelectronic MUX and DEMUX presented in this thesis may be viable approaches for building an entire high bit rate Optoelectronic TDM system.

REFERENCES

1 T. Kamiya , I Tanaka, and H. Kamiya, "GaAs integrated optoelectronic gating circuit suitable for 10 Gb/s demultiplexing," Proceedings of the Conference on Lasers and Electro-Optics 1987.

2 R.S. Tucker, G Eisenstein, S.K. Korotky, L.L. Buhl, J.J. Veselka, G. Raybon, B.L. Kasper, R.C. Alferness, "16 Gbit/s Fibre Transmission Experiment using Optical Time-Division Multiplexing," Elect. Lett. vol. 23, pp. 1270-1271, 1987.

3 A.H., Gnauck, S.K. Korotky, B.L. Kasper, J.C. Campbell, J.R. Talman, J.J. Veselka, A.R. McCormick, "Information bandwidth limited transmission at 8 Gb/s over 68.3 Km of single mode fiber," Digest of technical papers, Conference on optical fibre communications, Atlanta, 1986, Paper PDP6.

4 S. Fujita, N. Henmi, I. Takano, M. Yamaguchi, T. Torikai, T. Suzaki, S. Takano, H. Ishihara, and M. Shikada, "A 10 Gbit/s-80 km optical fiber transmission experiment using a directly modulated DFB-LD and a high speed InGaAs-APD," Optical Fibre Comm. Conf., New Orleans, LA, Jan. 1988, postdeadline paper PD16.

5 G. Eisenstein, R.S. Tucker, G. Raybon, "Optical Time-Division Multiplexed Transmission at 8 Gbit/s using Single Laser and Semiconductor Optical Power Amplifier," Electr. Lett., Vol. 25, No. 16, pp. 1034-1036. 1989.

6 G. Eisenstein, R.S. Tucker, U. Koren, and S.K. Korotky, "Active mode-locking characteristics of InGaAsP-single mode fiber composite cavity lasers," IEEE J. Quantum Electron., vol. QE-22, pp. 142-148, 1985.

7 J. Auyeung, "Picosecond optical pulse generation at gigahertz rates by direct modulation of a semiconductor laser," App. Phys. Lett., vol. 38, pp. 308-310, 1981.

8 R.S. Tucker, G. Eisenstein, S.K. Korotky, "Optical Time-Division Multiplexing for very High Bit Rate Transmission," J. of Ligthwave Tech., Vol 16, No. 11, pp. 1737-1749, 1988.

9 K.P. Jackson, and colleagues, "Optical Fibre Delay-Line Signal Processing," IEEE Trans. on Microw. Theory and Tech., Vol. MTT-33, pp. 193-209, 1985.

10 K.O. Hill, B.S. Kawasaki, and D.C. Johnson, "Efficient power combiner for demultiplexing multiple sources to single-fibre optical systems," Appl. Phys. Lett., Vol. 31, pp. 740-742, 1977.

11 Edited by S.E. Miller and I.P Kaminow, "Optical Fiber Telecommunications 2, San Diego: Academic Press, p. 734, 1988.

12 S. Hamilton, "Shunt Mode Harmonic Generation using Step Recovery Diodes," Microwave Journal, pp. 69-78, 1967.

13 "Pulse and Waveform Generation with Step Recovery Diodes," Hewlett Packard, Application note 918.

14 R.I. MacDonald, E.H. Hara, "Optoelectronic Broadband Switching Array," Electron. Lett., 16, pp. 502-503, 1978.

15 R.I. MacDonald and E.H. Hara, "Switching with Photodiodes," IEEE J. of Quantum Elect., vol. QE-16, pp 289-295, 1980.

16 H. Kanbe, N. Susa, H. Nakagome, and H. Ando, "InGaAs avalanche photodiode with InP p-n junction," Electron. Lett., vol. 16, pp.163-165, 1980.

17 R. A. Kiehl and D. M. Drury, "An optically-coupled microwave switch," IEEE Int. Microwave Symposium Digest., pp 314-316, 1980.

18 E. H. Hara, S. Machida, M. Ikeda, H. Kanbe, and I. Kimura, "Optoelectronic matrix switch using heterojunction switching photodiodes," Elect. Lett., vol. 17, pp. 150-151, 1981.

19 S.R. Forrest, G.L. Tangonan, and V. Jones, "A Simple 8 X 8 Optoelectronic Crossbar Switch," J. of Lightwave Technology, vol. 7, pp 607-614, 1989.

20 T. Sugeta, T. Urisu, S. Sakata, and Y Mizushima, "Metal Semiconductor-Metal Photodetector of for High-Speed Optoelectronic Circuits," Musashimo Electric Communication Laboratories, Nippon Telegraph and Telephone Public Corporation, Musashimo-shi, Tokyo, 180 Japan, 1979.

21 S.M. Sze, Physics of Semiconductor Devices. New York: Wiley-Interscience, 1981.

22 P.K. Cheo, Fiber Optics: Devices and Systems. Englewood Cliffs: Prentice Hall, p. 289, 1980.

APPENDIX A

EQUIPMENT USED

This appendix lists the brand name and type of equipment referred to in the thesis.

Multimeter	Fluke 75.
Network analyzer	Hewlett Packard 8753A with 85046 S-Parameter Test Set.
Package	Triquint FP-10.
Pattern generator / Error detector	Hewlett Packard 3780A
Power meter	Newport Corporation, 835 Optical Power Meter.
Pulse generator	AVTECH AVN-3-P.
Scope	Tektronix 7104, 7A29 Amplifier, 7B10 Time base.
Spectrum analyzer	Hewlett Packard 3585A
Test jig	Triquint ETF-FP10.

APPENDIX B

DEVICE DATA SHEETS

This appendix contains the data sheet for the Mitsubishi ML6411A laser and the ANTEL SL1002 PIN diode.

MITSUBISHI LASER DIODES

ML6101A,ML6411A ML6701A

FOR OPTICAL INFORMATION SYSTEMS

DESCRIPTION

Mitsubishi ML6101A, ML6411A, ML6701A are AlGaAs high power laser diodes emitting light beams around 780 nm wavelength. They lase by applying forward current exceeding threshold values, and emit light power about 10 mW CW at operating current around 25 mA in excess of the threshold current.

They operate, under CW or pulse condition according to input current, at case temperature up to 60°C.

Since they lase in a stable fundamental transverse mode, TE_{00} and smooth, linear light vs. current characteristics, they are well suited for optical information processing systems, and other optical system.

APPLICATION

- Writing and reading memory discs
- Laser cards
- laser printers ,

Under pulsed condition, such as disc memory writing, a peak light output of 25 mW can be obtained.

The ML6101A, ML6411A, ML6701A are hermetically sealed devices having a silicon photodiode for monitoring the light output.

Output current of the photodiode can be used for automatic control of the operating currents or case temperature of the lasers.

FEATURES

- Low threshold current, typical 40mA
- CW or pulsed operation up to case temperature of 60°C
- Electrical monitoring (a photodiode is installed in the laser package)

OUTLINE DRAWINGS Dimensions in mm

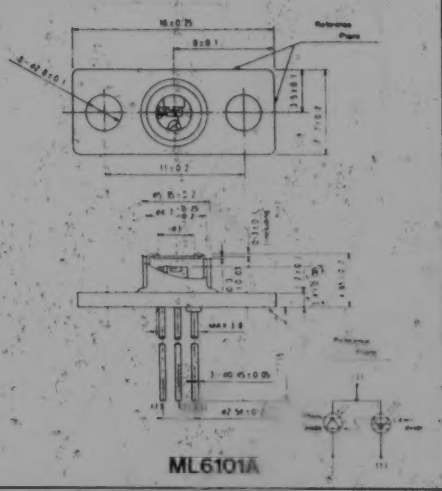

ML6101A

OUTLINE DRAWINGS Dimensions in mm

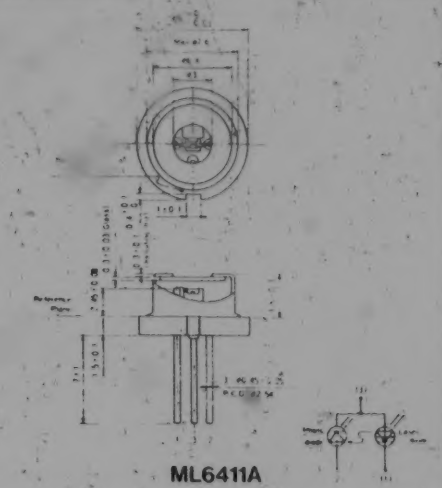

ML6411A

B.1 Data sheet for the Mitsubishi ML6411A laser

MITSUBISHI LASER DIO

ML6101A,ML641
ML6701A

FOR OPTICAL INFORMATION SYSTE

OUTLINE DRAWINGS

Dimensions in mm

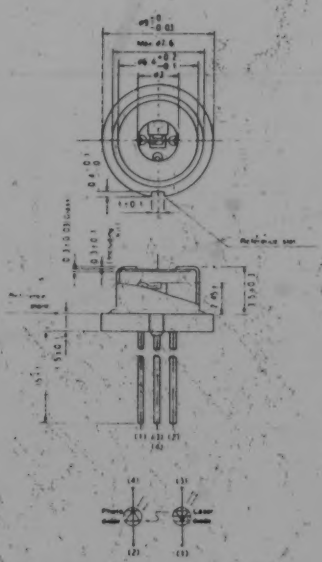

ML6701A

ABSOLUTE MAXIMUM RATINGS

Symbol	Parameter	Conditions	Ratings	Unit
P_O	Light output (peak)	CW	20	mW
		Pulse (Note1)	25	
V_{RL}	Reverse voltage (Laser diode)	–	2	V
V_{RD}	Reverse voltage (Photodiode)	–	15	V
I_{FD}	Forward current (Photodiode)	–	10	mA
T_C	Operating case temperature	–	−40 ~ +60	°C
T_{stg}	Storage temperature	–	−55 ~ +100	°C

Note1 : Duty less than 50%, pulse width less than 1μs.

ELECTRICAL/OPTICAL CHARACTERISTICS (T_c=25°C)

Symbol	Parameter	Test conditions	Characteristics			Unit
			Min.	Typ.	Max.	
I_{th}	Threshold current	CW	15	40	60	mA
I_{op}	Operating current	CW, P_O=10mW	–	65	100	mA
V_{op}	Operating voltage (Laser diode)	CW,P_O10mW	–	2.0	2.5	V
I_D	Dark current (Photodiode)	V_{RD}=10V	–	–	0.5	μA
P_O	Light output	CW, $I_F = I_{th}$ + 25mA	–	10	–	mW
λ_p	Lasing wavelength	CW,P_O=10mW	765	780	795	nm
$\theta_{\parallel}$	Full angle at half maximum	CW, P_O=10mW	10	12	17	deg
$\theta_{\perp}$			20	30	35	deg
C_t	Capacitance (Photodiode)	V_R=0V, f=1MHz	–	7	–	pf
I_m	Monitoring output current	CW,P_O=10mW V_{RD}=1V R_L=10Ω (Note2)	0.3	0.8	1.7	mA

Note2 R_L is load resistance of the photodiode

1. Light output vs forward current

Typical light output vs forward current characteristics are shown in Fig. 1. The typical threshold current for lasing is 40 mA at room temperature. Above the threshold, the light output increases linearly with current, and no kinks are observed in the curves. As can be seen in Fig. 1, the threshold current and slope efficiency (dP_O/dI_F) depends on case temperature of the lasers.

This suggests that an automatic control of temperature or current is necessary to keep the light output constant since temperature variation is inevitable in practical systems. The automatic controls should be such that the maximum ratings of the light output and the case temperature are not exceeded. "OPERATING CONSIDERATIONS" gives an example of the automatic light output control circuit.

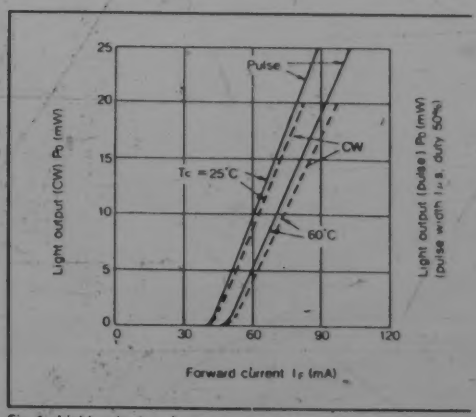

Fig. 1 Light output vs forward current

2. Temperature dependence of threshold current (I_{th}), operating current (I_{op}) and slope efficiency (η_O)

A typical temperature dependence of the threshold current and the operating current at 10mW are shown in Fig. 2. The characteristics temperature To of the threshold current is typically 180K in $T_C \leqq 50°C$ where the definition of T_O is $I_{th} \propto \exp(T_C/T_O)$.

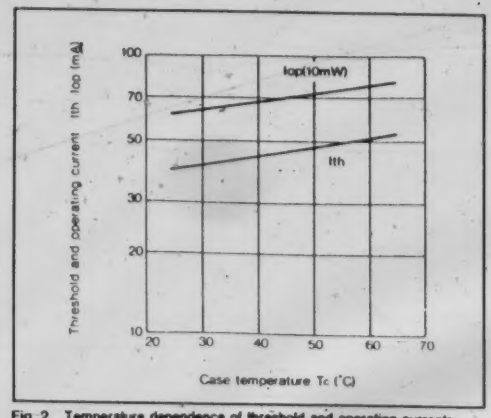

Fig. 2 Temperature dependence of threshold and operating currents

A typical temperature dependence of the slope efficiency η_O is shown in Fig. 3. The gradient is -0.001mW/mA/°C typ.

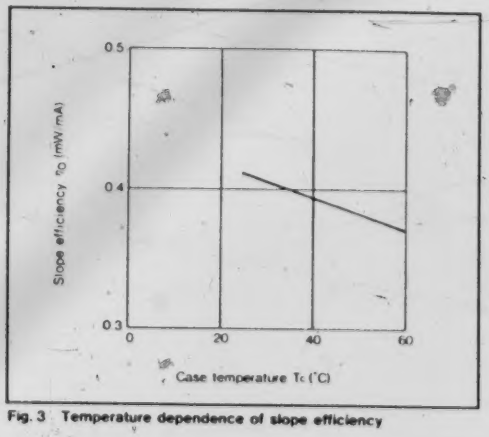

Fig. 3 Temperature dependence of slope efficiency

3. Forward current vs voltage

Typical forward current vs voltage characteristics are shown in Fig. 4. In general, as the case temperature rises, the forward voltage V_f decreases slightly at a constant current I_f. V_f varies typically at a rate of -2.0 mV/°C at $I_f = 1mA$.

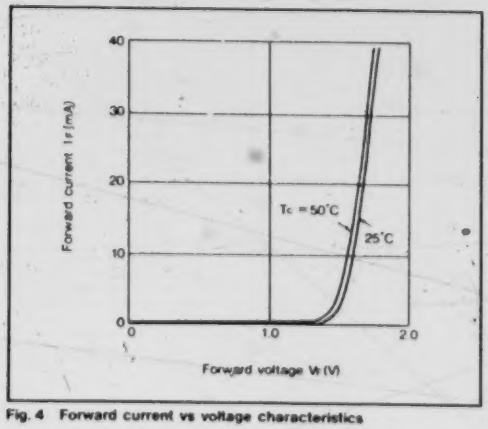

Fig. 4 Forward current vs voltage characteristics

4. Emission spectra

Typical emission spectra under CW operation are shown in Fig. 5. In general, at an output of 20mW, single mode is observed. The peak wavelength depends on the operating case temperature and the forward current (output level).

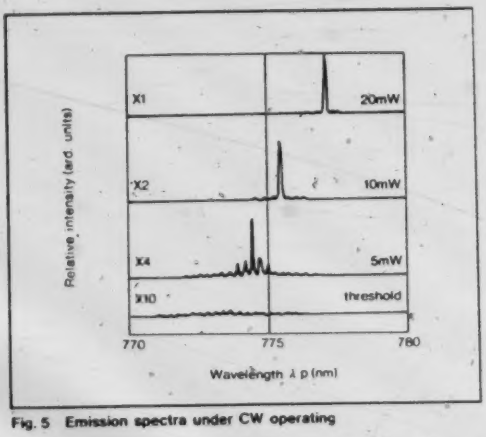

Fig. 5 Emission spectra under CW operating

A typical temperature dependence of the peak wavelength at an output of 10mW is shown in Fig. 6.
The peak wavelength of the beam shifts and jumps to adjacent longitudinal mode by variation of operating temperature.
Averaged temperature coefficient which includes the shifts and jumps is about 0.25 nm/°C.

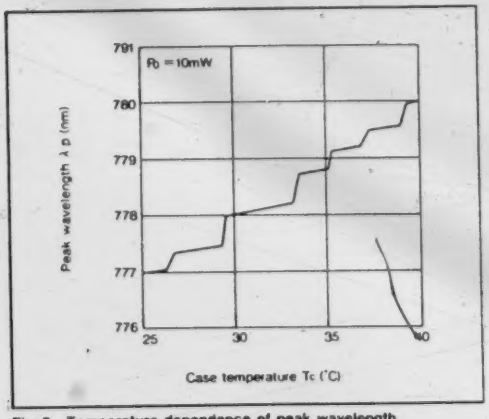

Fig. 6 Temperature dependence of peak wavelength

5. Far-field radiation pattern

The ML6101A, ML6411A, ML6701A laser diodes lase in fundamental transverse (TE_{00}) mode and the mode does not change with the current. They have a typical emitting area (size of near-field pattern) of 0.7 x 2.5μm^2. Fig. 7 and Fig. 8 show typical far-field radiation patterns in "parallel" and "perpendicular" planes, respectively. The full angles at half maximum points (FAHM) are typically 12° and 30°, respectively.

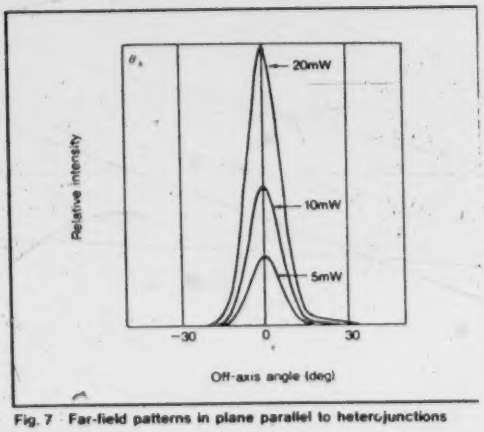

Fig. 7 Far-field patterns in plane parallel to heterojunctions

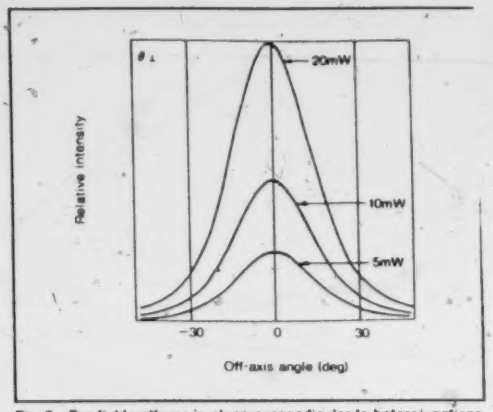

Fig. 8 Far field patterns in plane perpendicular to heterojunctions

6. Pulse response

In the digital optical transmission systems, the response waveform and speed of the light output against the input current pulse waveform (shown in Fig. 9 upper) is one of main concerns. The speed depends on the oscillation delay time, rise and fall times. In order to shorten the oscillation delay time, the laser diode is usually biased close to the threshold current since the delay time is a time for charging the junction up to the threshold. Fig. 9 shows the typical response waveform when rectangular pulse current is applied.

The rise and fall times are typically 0.3ns and 0.4ns, respectively. They are limited by response speed of the detector.

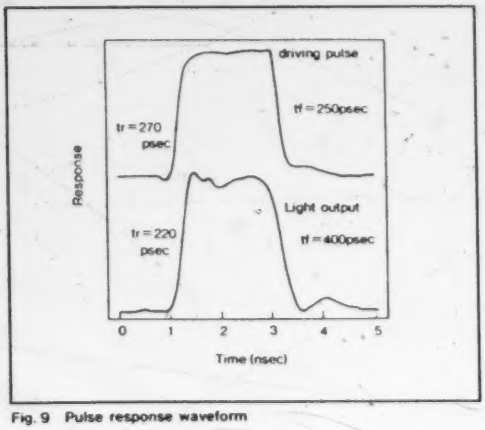

Fig. 9 Pulse response waveform

7. Monitoring output

The laser diodes emit beams from both of their mirror surfaces, front and rear surfaces (see the outline drawing). The rear beam can be used for monitoring power of front beam since the rear beam is proportional to the front one. In the case of ML6101A, ML6411A, ML6701A lasers, the rear beam powers are changed into photocurrents by the monitoring photodiodes. Fig. 10 shows an example of light output vs monitoring photocurrent characteristics. Above the threshold, the monitored photocurrent linearly increases with the light output.

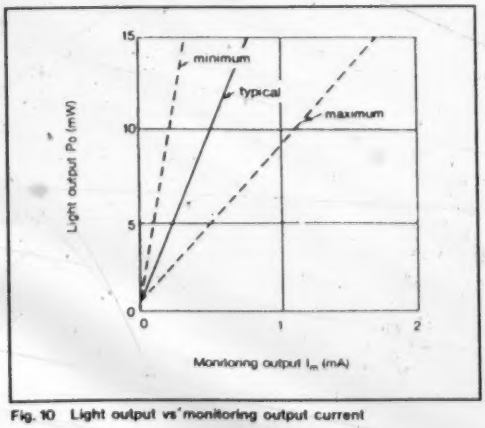

Fig. 10 Light output vs monitoring output current

8. Polarization ratio

The polarization ratio ($P_{\perp}/P_{\parallel}$), which is the ratio of the parallel polarized light output and the perpendicular polarized one, vs. total light output characteristics is shown in **Fig. 11**. The polarization ratio linearly increases with the light power.

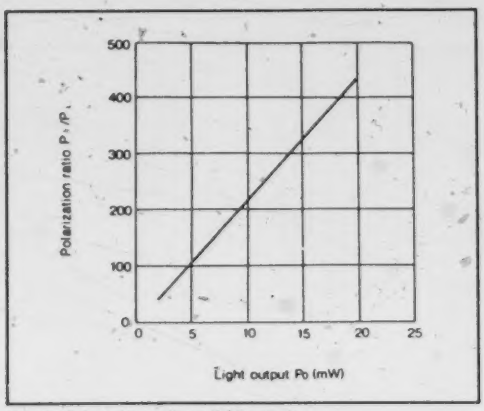

Fig. 11 Polarization ratio vs light output

9. Impedance characteristics

Typical impedance characteristics of the ML6101A, ML6411A, ML6701A lasers, with lead lengths of 2mm, is shown in **Fig. 12** with the bias currents as the parameter. Test frequency is swept from 100MHz to 1300MHz with 100MHz step.

Above the threshold, the impedance can be approximated by a series connection of a resistance of 3 ohm and an inductance of 3nH.

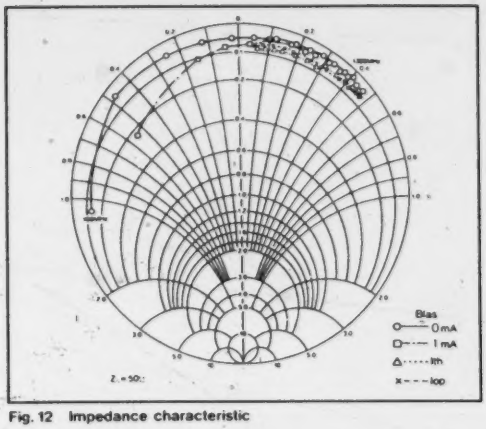

Fig. 12 Impedance characteristic

10. S/N vs optical feedback ratio

The signal to noise (S/N) of the laser beam is defined as the DC to noise electric power ratio after changing the laser beam to electric signal. Therefore, the defined S/N corresponds to square of the DC/noise optical power ratio.

Fig. 13 shows the S/N vs the optical feedback at the frequency of 10MHz and with the bandwidth of 300kHz.

Fig. 14 shows similar characteristics at a low frequency, 20kHz, and with the bandwidth of 300Hz.

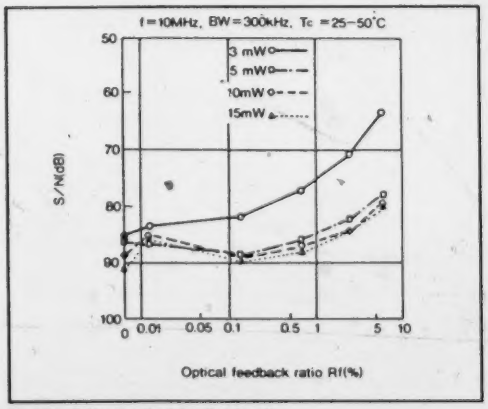

Fig. 13 S/N vs optical feedback ratio

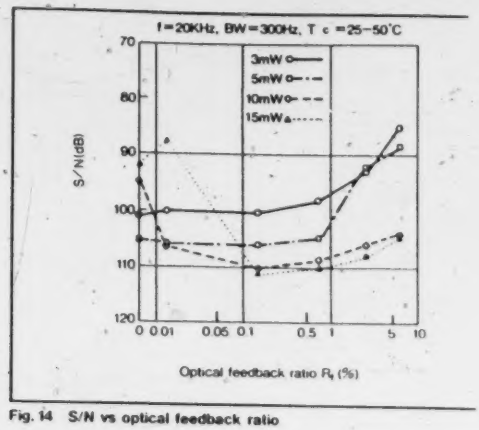

Fig. 14 S/N vs optical feedback ratio

LASER DIODE TEST DATA

Model No.: PT-150
Serial No.: 1366
Wavelength: 776 nm
Laser Type: MITSUBISHI ML6411C

Rated Po: 4765 micro W
Date tested: Dec 11, 1989
Tested by: Howard Lo

POWER OUTPUT VS. FORWARD CURRENT

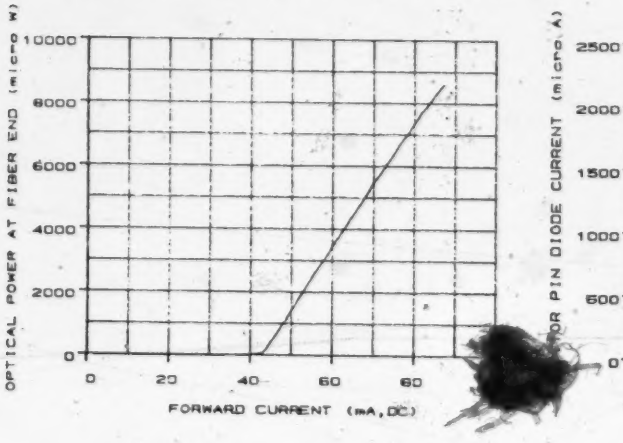

PIN CURRENT VS. OUTPUT POWER

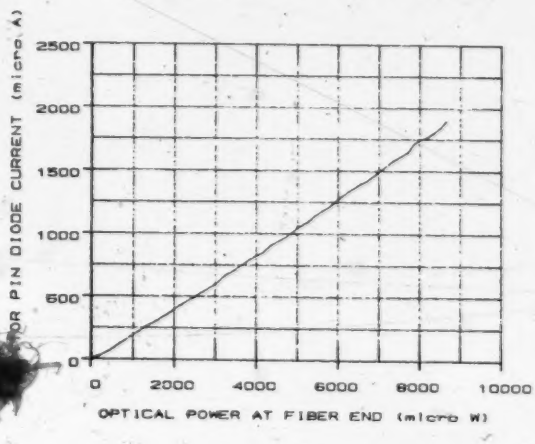

ANTEL
OPTRONICS INC.

HIGH PERFORMANCE
SILICON & GERMANIUM LASER MONITOR PHOTODIODES

TYPES: SL1002, SL1005, SL1010, GL1002, GL1005, GL1010

TECHNICAL DATA APRIL 1987

Features

- Low Voltage Operation
- High Speed Response
- High Reliability
- Low Dark Current
- Wide Spectral Response

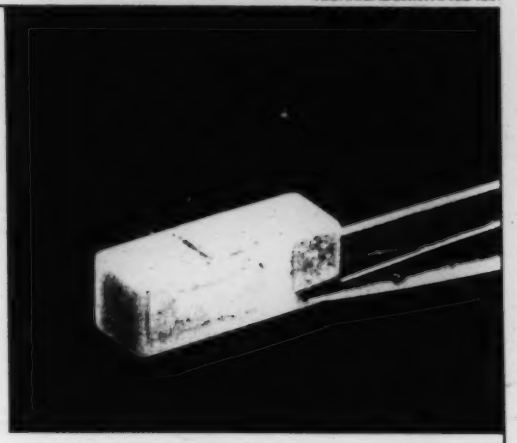

Applications

- Laser Feedback
- LED Monitors
- FO Receivers

Description

The high performance line of ceramic mounted Silicon and Germanium PIN photodiodes are designed specifically for employment in Fiber Optic Transmitter and receiver Modules. They offer a unique combination of high sensitivity, low noise and fast speed of response. Stringent quality control and proprietary device passivation ensures a high degree of reliability.

Package Dimensions

SMC-TYPE

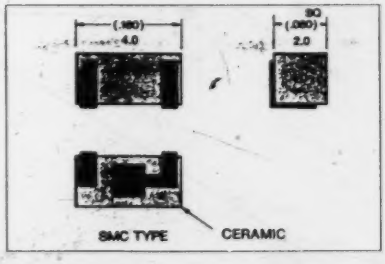

Ceramic Submount

Material: Alumina
Metalization: Ni/Au
Chip Bond: Eutectic/Epoxy

Dimensions in millimeters. Dimensions in parentheses are in inches.
Note: Optional & Custom ceramic packages are also available.

To order or for further information call:

ANTEL
OPTRONICS INC.
3329 MAINWAY•BURLINGTON, ONTARIO•CANADA•L7M 1A6
TELEPHONE 416/335-3207 TELEX 06-[illegible] FAX 416/335-1183

Antel Optronics Inc. reserves the right, without notice, to make changes in equipment design or specifications. Information supplied by Antel Optronics is believed to be accurate and reliable. However, no responsibility is assumed by Antel Optronics Inc. for its use nor for any infringement of patents or other rights of third parties which may result from its use.

REFERENCE NO. 103

B.2 Data sheet for the ANTEL SL1002 PIN diode

Mechanical Characteristics

Silicon Series Part Number	Photosensitive Surface		Package[1] Description	Germanium Series Part Number	Photosensitive Surface	
	Dia. mm	Area mm²			Dia. mm	Area mm²
SL1002	0.2	0.03	Ceramic SMC Type	GL1002	0.2	0.03
SL1005	0.5	0.20		GL1005	0.5	0.20
SL1010	1.0	0.80		GL1010	1.0	0.80

Absolute Maximum Ratings

Parameter	Silicon Series Maximum Ratings	Germanium Series Maximum Ratings	Units
DC Reverse Voltage	125	18	volts
Photocurrent Density Average Value Peak value	5 25	8 30	mA/mm² mA/mm²
Forward Current Average value, continuous operation Peak value	10 100	20 200	mA mA
Ambient — operating — storage	-60 to +80 -60 to +150	-55 to +75 -55 to +125	°C °C
Soldering	200	200	°C

Electrical/Optical Characteristics at[2] $T_A = 22°C$ $V_R = -12$ volts

Part Number	Spectral Response	Radiant Sensitivity Typical (A/W)		N.E.P. @ 900 nm	Dark Current	Minimum Breakdown	Capicitance @ 1000 Hz	Cutoff frequency λ = 900 nm R_L = 50 Ω
	10% Points	@ 900 nm	@ 1300 nm	W/√Hz	(nA)	Voltage (volts)	(pF)	(MHz)
SL1002	400 - 1100	.45	—	1×10^{-13}	0.05	125	0.5	2.0
SL1005	400 - 1100	.45	—	1×10^{-13}	0.10	125	0.75	1.5
SL1010	400 - 1100	.45	—	1×10^{-13}	0.50	125	1.10	1.0
					(uA)			(MHz λ = 1300nm)
GL1002	500 - 1800	.40	.75	1×10^{-13}	1.0	20	2.5	300
GL1005	500 - 1800	.40	.75	1×10^{-13}	2.5	18	10	200
GL1010	500 - 1800	.40	.75	1×10^{-12}	10	18	30	100

NOTES:
1. The operational range is 0 to -15 volts.
   When the device is operated in the photovoltaic mode at V_R = 0 volts, some of the electrical characteristics will differ from those shown.
2. Devices can also be supplied on custom packages.
3. Standard high voltage, high responsivity Silicon PIN Diodes are also available.

Silicon PIN Photodiode Series

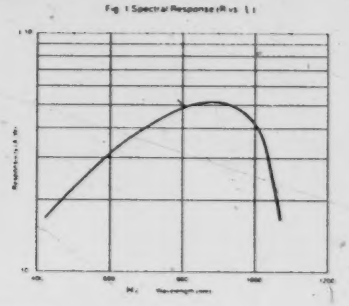

FIGURE #1

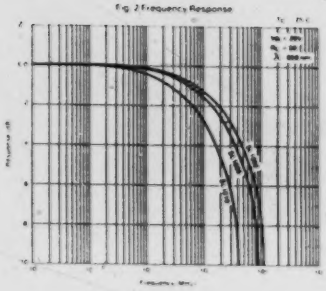

FIGURE #2

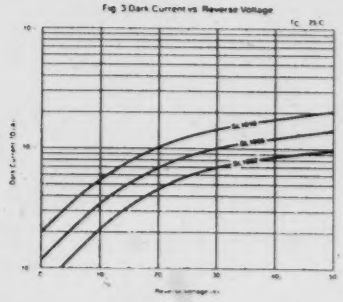

FIGURE #3

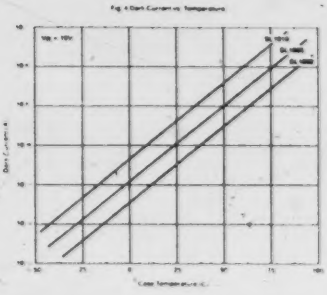

FIGURE #4

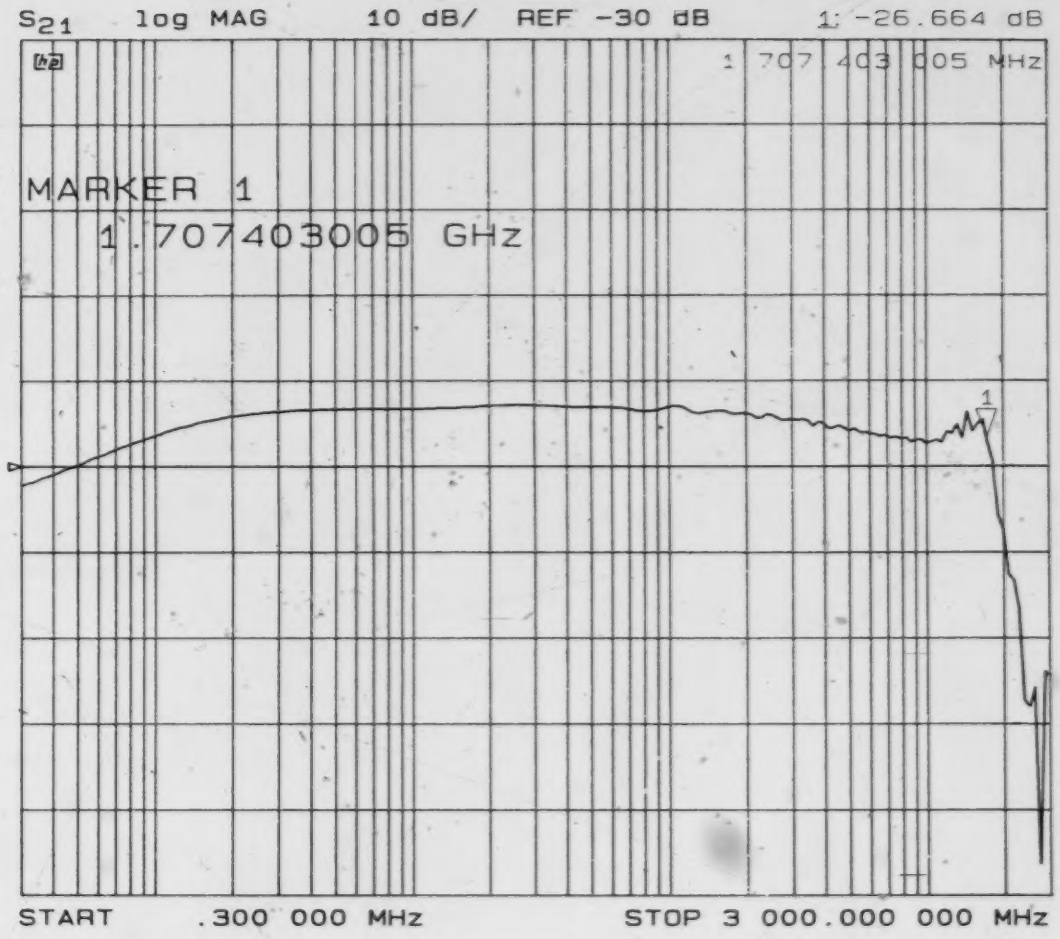

Fig. B1 PIN detector frequency response, $R_1 = 50$ ohms.

APPENDIX C

CIRCUIT SCHEMATICS AND FREQUENCY RESPONSES

This appendix contains the circuit schematic of the:

-shift register module,

-power splitter / phase shifter module,

-ECL to TTL converter,

-70 MHz low pass filter,

-and the differential amplifier.

It also contains the frequency response of :

-amplifiers 1 and 3,

-the low pass filter,

-and the differential amplifier.

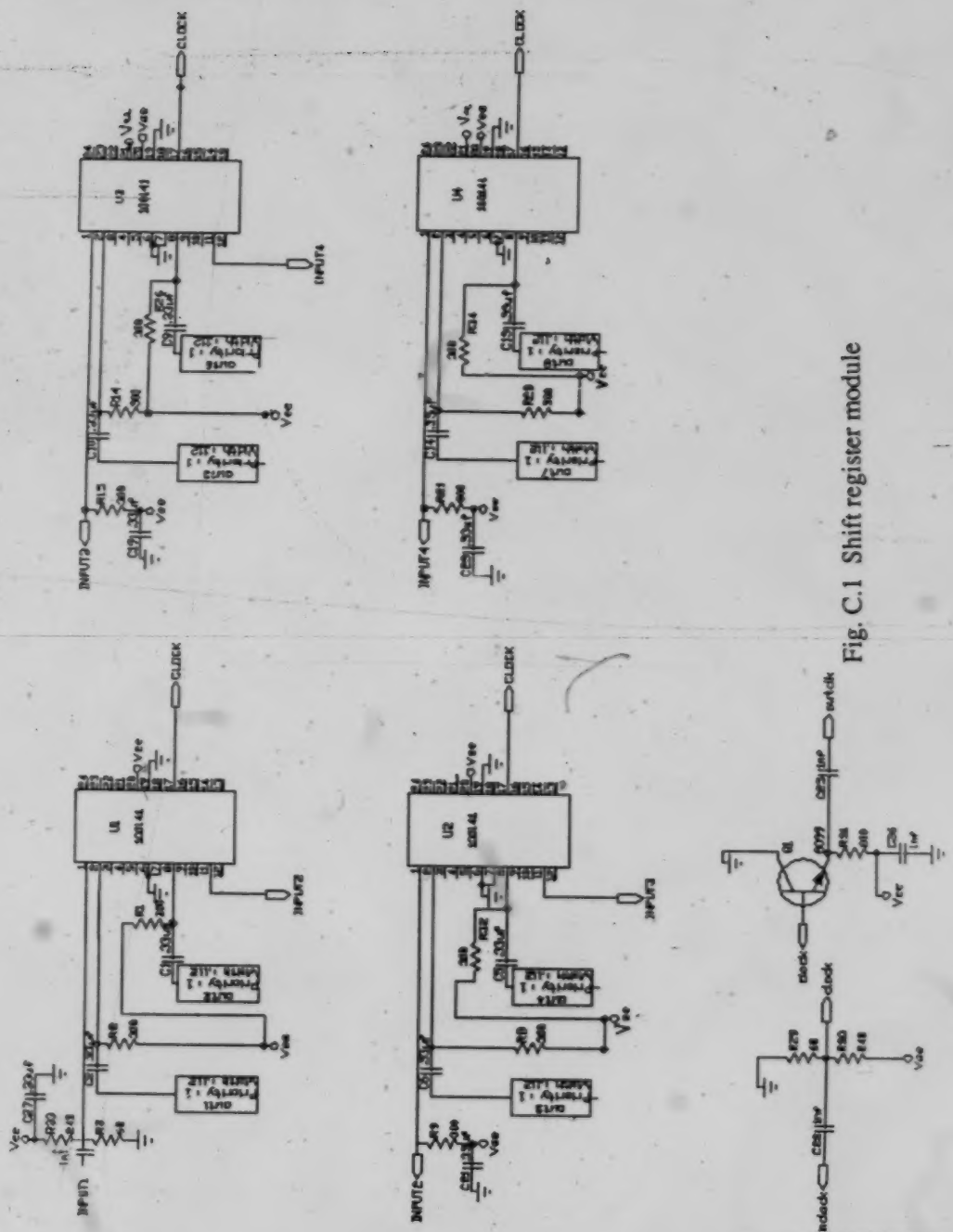

Fig. C.1 Shift register module

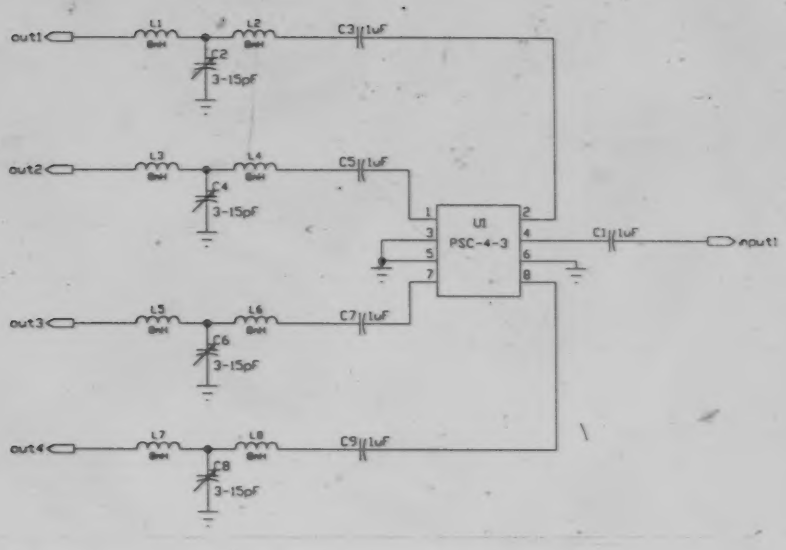

Fig. C.2 Power splitter / phase shifter.

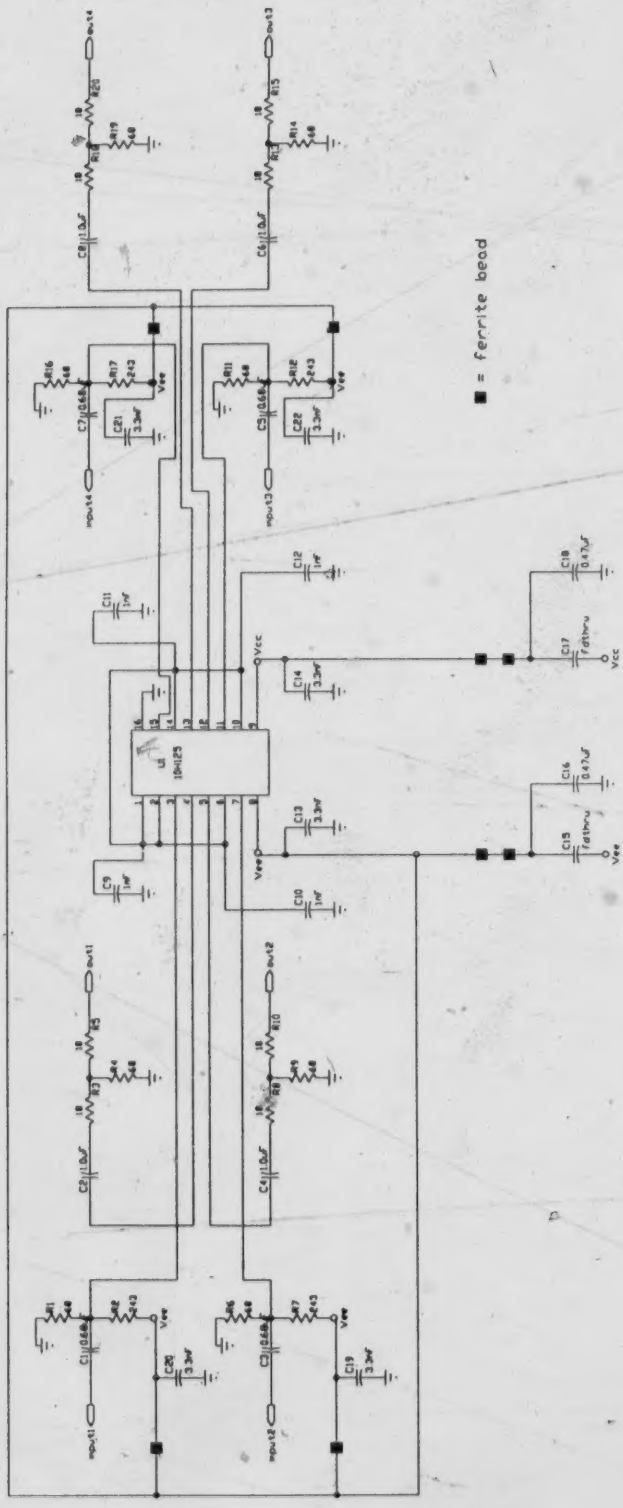

Fig. C.3 EC L to TTL converter

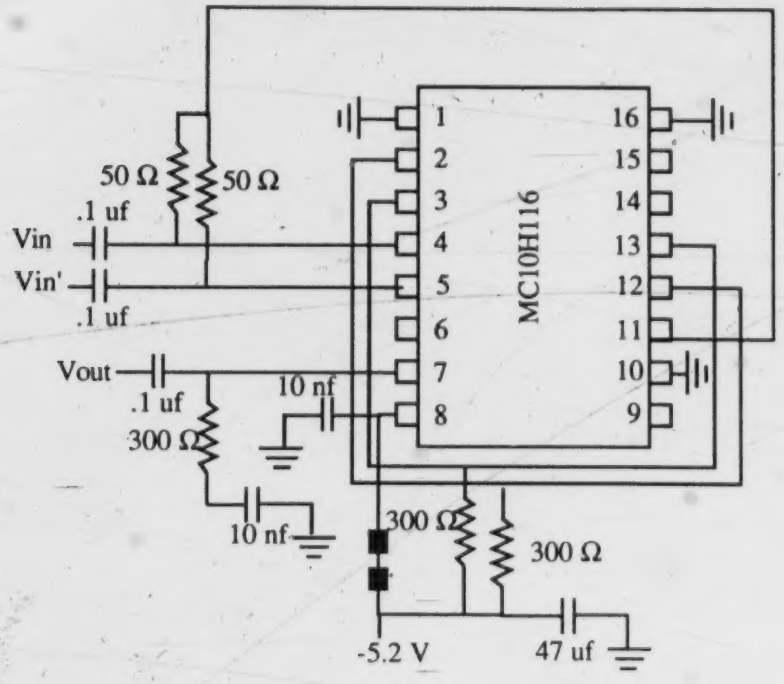

Fig. C.4 Differential amplifier.

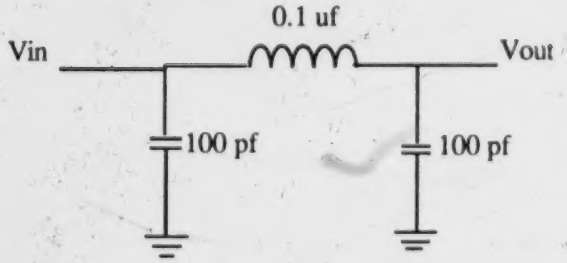

Fig. C.5 Third order Butterworth low pass filter.

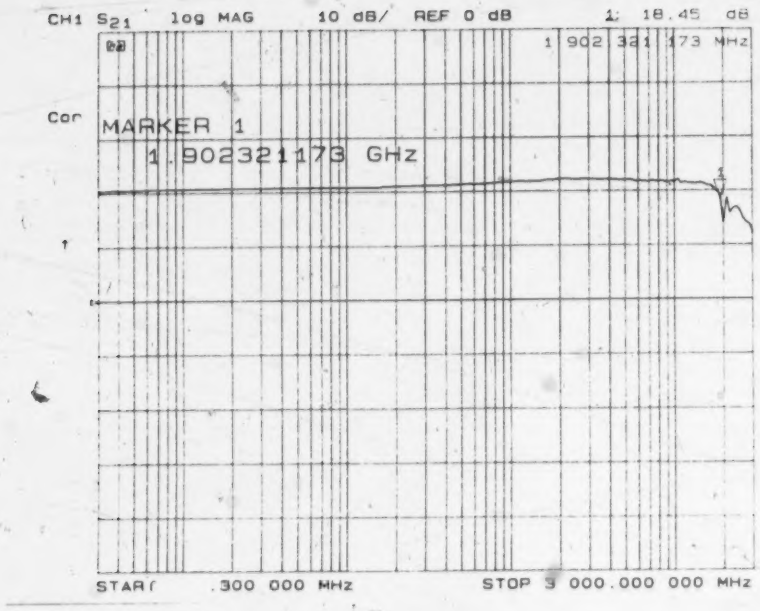

Fig. C.6 Amp. 1 frequency response.

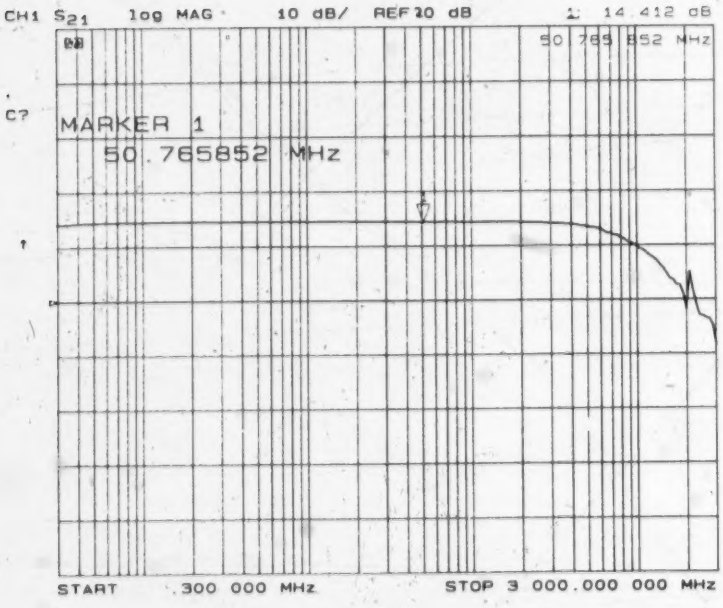

Fig. C.7 Amp. 3 frequency response

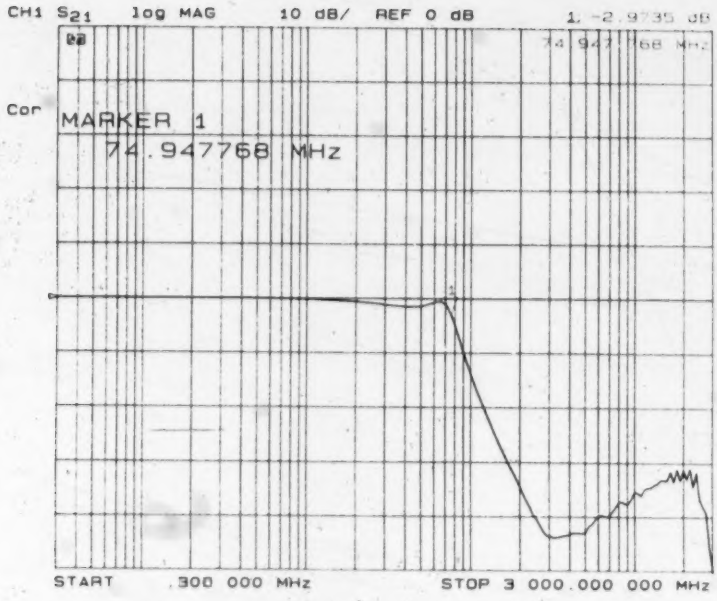

Fig. C.8 LPF frequency response.

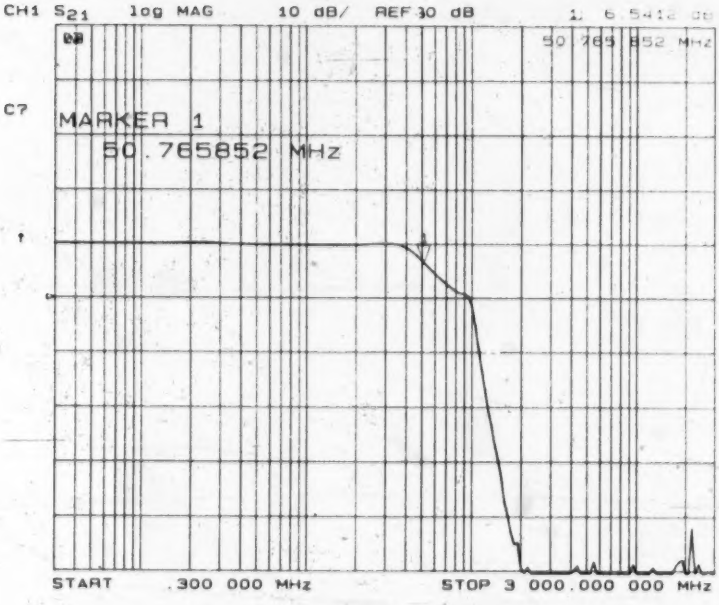

Fig. C.9 Differential amp. frequency response